optica

Third-generation femtosecond technology

Hanieh Fattahi,[1,2] Helena G. Barros,[2] Martin Gorjan,[1,2] Thomas Nubbemeyer,[2] Bidoor Alsaif,[1,3,4] Catherine Y. Teisset,[5] Marcel Schultze,[5] Stephan Prinz,[5] Matthias Haefner,[5] Moritz Ueffing,[2] Ayman Alismail,[2,3] Lénárd Vámos,[2,6] Alexander Schwarz,[1,2] Oleg Pronin,[2] Jonathan Brons,[2] Xiao Tao Geng,[1,7] Gunnar Arisholm,[8] Marcelo Ciappina,[1] Vladislav S. Yakovlev,[1,2,9] Dong-Eon Kim,[7] Abdallah M. Azzeer,[3] Nicholas Karpowicz,[1] Dirk Sutter,[10] Zsuzsanna Major,[1,2] Thomas Metzger,[5] and Ferenc Krausz[1,2,*]

[1]Max-Planck Institut für Quantenoptik, Hans-Kopfermann-Str. 1, D-85748 Garching, Germany

[2]Department für Physik, Ludwig-Maximilians-Universität München, Am Coulombwall 1, D-85748 Garching, Germany

[3]Physics and Astronomy Department, King Saud University, Riyadh 11451, Saudi Arabia

[4]Current address: Electrical Engineering, Computer, Electrical and Mathematical Sciences and Engineering Division, Building 1, 4700 King Abdullah University of Science and Technology, Thuwal 23955-6900, Saudi Arabia

[5]TRUMPF Scientific Lasers GmbH + Co. KG, Feringastr. 10, 85774 München-Unterföhring, Germany

[6]Wigner Research Center for Physics, Konkoly-Thege Miklós út 29-33, H-1121 Budapest, Hungary

[7]Physics Department, POSTECH, San 31 Hyoja-Dong, Namku, Pohang, Kyungbuk 790-784, South Korea

[8]FFI (Norwegian Defence Research Establishment), Postboks 25, NO-2027 Kjeller, Norway

[9]Current address: Center for Nano-Optics (CeNO), Georgia State University, Atlanta, Georgia 30303, USA

[10]TRUMPF Laser GmbH + Co. KG, Aichhalder Str. 39, 78713 Schramberg, Germany

*Corresponding author: krausz@lmu.de

Received 23 May 2014; revised 25 June 2014; accepted 26 June 2014 (Doc. ID 212665); published 22 July 2014

Femtosecond pulse generation was pioneered four decades ago using mode-locked dye lasers, which dominated the field for the following 20 years. Dye lasers were then replaced with titanium-doped sapphire (Ti:Sa) lasers, which have had their own two-decade reign. Broadband optical parametric amplifiers (OPAs) appeared on the horizon more than 20 years ago but have been lacking powerful, cost-effective picosecond pump sources for a long time. Diode-pumped ytterbium-doped solid-state lasers are about to change this state of affairs profoundly. They are able to deliver 1 ps scale pulses at kilowatt-scale average power levels, which, in thin-disk lasers, may come in combination with terawatt-scale peak powers. Broadband OPAs pumped by these sources hold promise for surpassing the performance of current femtosecond systems so dramatically as to justify referring to them as the next generation. Third-generation femtosecond technology (3FST) offers the potential for femtosecond light tunable over several octaves, multi-terawatt few-cycle pulses, and synthesized multi-octave light transients. Unique tunability, temporal confinement, and waveform variety in combination with unprecedented average powers will extend nonlinear optics and laser spectroscopy to previously inaccessible wavelength domains, ranging from the far IR to the x-ray regime. Here we review the underlying concepts, technologies, and proof-of-principle experiments. A conceptual design study of a prototypical tunable and wideband source demonstrates the potential of 3FST for pushing the frontiers of femtosecond and attosecond science.

OCIS codes: (140.0140) Lasers and laser optics; (140.3480) Lasers, diode-pumped; (190.4970) Parametric oscillators and amplifiers; (320.7160) Ultrafast technology; (140.3615) Lasers, ytterbium; (230.4480) Optical amplifiers.

http://dx.doi.org/10.1364/OPTICA.1.000045

1. INTRODUCTION

Femtosecond technology was born in the 1970s, when passively mode-locked dye lasers produced the first pulses shorter than 1 ps [1–3]. Subsequent advances led to pulse durations of a few tens of femtoseconds directly from laser oscillators [4–7]. The poor energy storage capability of laser dyes limited amplification to microjoule energies and megawatt peak powers [8,9]. This first-generation femtosecond technology (1FST) opened the door for direct time-domain investigations of hitherto immeasurably fast processes such as molecular dynamics, chemical reactions, and phase transitions in condensed matter [10,11].

Broadband solid-state lasers with large energy storage capabilities appeared by the end of the 1980s [12–14]. They offered the potential for further pulse shortening as well as boosting the pulse energy and peak power by many orders of magnitude. Second-generation femtosecond technology (2FST), based on chirped-pulse amplification (CPA) [15] in solid-state lasers, in particular, in Ti:sapphire-based systems [16–18], and dispersion control by chirped multilayer mirrors (henceforth, for brevity, chirped mirrors) [19–21] paved the way for the emergence of entirely new research fields and technologies such as attosecond science [22] and laser-driven particle acceleration [23].

2FST is now capable of providing pulses with ultrahigh (petawatt) peak power at moderate average power [24] and moderate-peak-power (gigawatt) pulses at ultrahigh (approaching the kilowatt scale) average power levels [25]; see Fig. 1. Based on optical parametric chirped-pulse amplification (OPCPA) [26] driven by terawatt-scale pulses from ytterbium lasers at kilowatt-scale average power, third-generation femtosecond technology (3FST) will, as a defining characteristic, *combine high (terawatt-scale) peak powers with high (kilowatt-scale) average powers* in ultrashort optical pulse generation for the first time. This unprecedented parameter combination will allow us to explore extreme nonlinearities of matter and extend ultrashort pulse generation to short (nanometer to subnanometer) as well as long (multimicrometer) wavelengths at unprecedented flux levels, holding promise for yet another revolution in ultrafast science. Figure 1 shows a summary of the performance of 1FST, 2FST, and 3FST systems.

OPCPA requires intense optical pulses for pumping the nonlinear medium used for the parametric conversion. The optimum duration of these pulses is of the order of 1 ps, constituting a trade-off between a high resistance to optical damage (decreasing for longer pulses [27–29]) and a small temporal walk-off [30,31] between pump and signal pulses relative to their duration (increasing for shorter pulses). OPCPA pumped by 1-ps-scale pulses offers octave-spanning light amplification with unprecedented efficiency, not accessible by any other technique known to date. Moreover, for very similar physical reasons, these pulse durations appear to be ideal for efficient frequency conversion of the pump light via low-order harmonic generation and/or frequency mixing [32,33]. Hence, a reliable, cost-effective, and power-scalable source of high-energy 1-ps-scale laser pulses would constitute the ideal basis

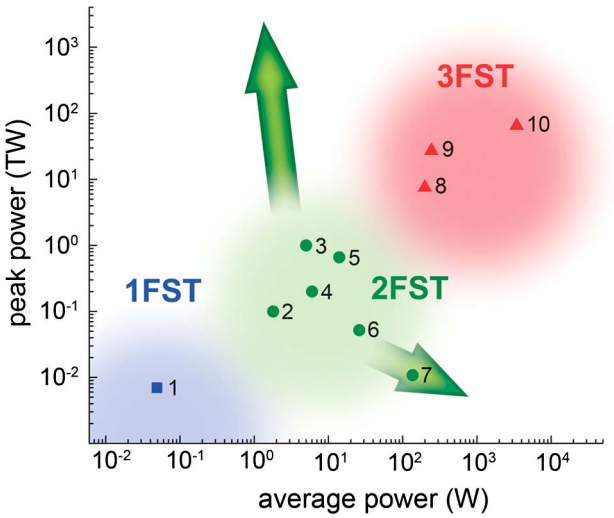

	τ_{pulse}	E_{pulse}	P_{peak}	$P_{average}$
system 8	5 fs	40 mJ	7.5 TW	200 W
system 9	1.7 fs	49 mJ	27 TW	245 W
system 10	5 fs	345 mJ	65 TW	3450 W

Fig. 1. Summary of recorded performances of 1FST and 2FST and the expected performance of 3FST, in terms of average and peak powers. These systems are reviewed in detail in Supplement 1. The blue square represents the best performance achieved by dye-laser technology (1, corresponding to Ref. [9]), the green dots show femtosecond CPA solid-state technology (2–7, corresponding to Refs. [60,71,66,18,67], and [25], respectively), and the red triangles represent the simulated results for OPCPA based on pump sources under development (8 and 9, pumped by a 1 ps, 5 kHz, 200 mJ Yb:YAG thin-disk laser) and envisioned (10, based on a future 1 ps, 10 kHz, 2 J Yb:YAG thin-disk laser system). Systems 8 and 10 use one OPCPA channel in the NIR, whereas in system 9 the output of three OPCPA channels in the VIS–NIR–IR are added for coherent synthesis of a subcycle waveform. The table summarizes the predicted output parameters of these systems. The relevant pump source architectures and multichannel OPCPA system are discussed in Section 2 and Section 3, respectively. OPCPA systems pumped by Yb:YAG slab and fiber amplifier systems [108,110] have been demonstrated in the performance range of 2FST and are not displayed in the figure.

for exploiting the full potential of OPCPA for ultrashort pulse amplification at a variety of wavelengths.

In this work we show that diode-pumped Yb-doped thin-disk lasers based on a technology well established in industrial environments fulfill all these requirements and offer a promising route to implementing 3FST in the conceptual architecture outlined in Fig. 2. In addition to simultaneously reaching peak and average power levels that will outperform 1FST and 2FST by several orders of magnitude (Fig. 1), 3FST systems allow a variety of operational modes, offering multicycle pulses tunable over several octaves, few-cycle pulses at different carrier wavelengths, and multi-octave synthesis of light waveforms.

Our discussion in this paper focuses on powerful ultrashort-pulse generation at high (≥1 kHz) repetition rates; ultrahigh-intensity lasers emitting a few pulses per second or less as well as sources delivering moderate-power pulses at high average power are out of the scope of this work (for a review, the

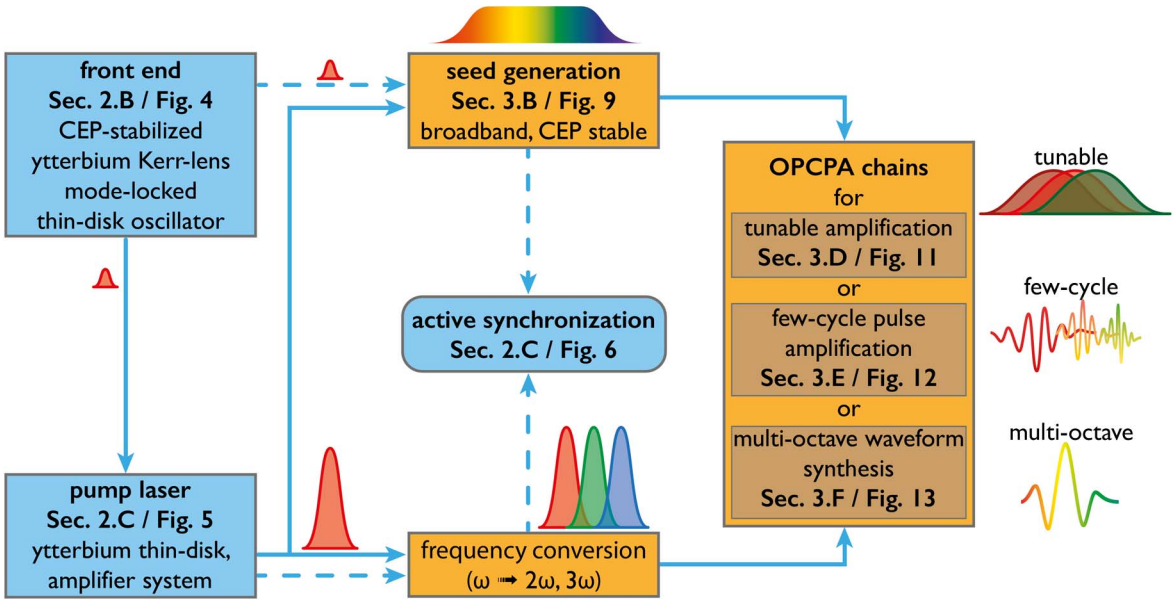

Fig. 2. Basic conceptual architecture of a 3FST system. A subpicosecond ytterbium laser oscillator seeds the pump source. The broadband seed can be generated either from the output of the picosecond pump laser (solid arrows) or directly from the oscillator (dashed arrows). In the latter case an active temporal synchronization is needed between the pump and seed pulses of the OPCPA chain. The 3FST source can be operated to generate (i) widely tunable pulses of a few tens of femtoseconds duration, (ii) few-cycle pulses in different spectral ranges, or (iii) multi-octave controlled waveforms with a sub-optical-cycle structure. The building blocks of the 3FST system are discussed in detail in the respective sections as indicated in the figure.

interested reader is kindly referred to relevant reviews in [23] and [34], respectively). A brief historical overview of 1FST [1–9,35–45] and 2FST [12–21,45–73] is presented in Supplement 1. The remaining part of the introduction addresses some of the major milestones of OPCPA history.

A. Conceptual Basis for 3FST

Optical parametric amplification (OPA) was discovered in the 1960s [74,75], but only nonlinear crystals with a high second-order nonlinear susceptibility and high resistance to optical damage, such as β-barium borate (BBO) [76] along with the invention of OPCPA by Piskarskas and co-workers [26] opened the prospect for efficient amplification of femtosecond laser pulses via this mechanism. A prerequisite for OPA being able to provide a competitive alternative to femtosecond laser amplifiers is the availability of power-scalable pump sources with a good wall-plug efficiency. So far, only lasers with pulse durations much longer than 1 ps have been able to meet this requirement. The instantaneous nature of the OPA pump-to-signal energy conversion calls for a signal pulse that is temporally stretched to match the duration of the pump pulse for efficient OPA and then recompressed after amplification.

The bandwidth of OPCPA can be enhanced by a noncollinear pump-signal beam propagation geometry, utilizing the slightly different propagation directions of the interacting beams to compensate the effect of material dispersion in the nonlinear medium [77,78]. Drawing on these basic concepts and a variety of pump and seed sources, a large number of OPA experiments aiming at efficient amplification of ultrashort pulses have been performed over the past 20 years. Their review is beyond the scope of this paper; we refer the interested reader to a number of excellent review articles on this subject [79–83].

OPCPA has been demonstrated to be capable of amplifying pulses as short as 4 fs [84], achieving peak-power levels of 16 TW from a tabletop system [85], approaching the petawatt frontier when pumped by large-scale lasers [86–92], and reaching average power levels as high as 22 W at a 1 MHz repetition rate [93]. However, none of these systems have been capable of achieving high peak and average powers simultaneously. The most powerful OPCPA system of this kind reported to date delivers 0.49 TW pulses at an average power of 2.7 W [94], which is still inferior to state-of-the-art Ti:Sa systems. The pump laser technology described in Section 2 holds promise for changing this state of affairs dramatically.

In what follows, Section 2 reviews near-1-ps pulse amplification and its implementation with thin-disk lasers, scalable to high peak as well as average powers. Section 3 is devoted to conceptual design studies demonstrating the potential of 3FST for creating a source of femtosecond light with unprecedented characteristics, and Section 4 addresses some of the expected implications.

2. NEAR-1-PS YTTERBIUM LASERS

Near-1-ps laser pulses with high peak power have long been available from flashlamp-pumped passively mode-locked neodymium-doped glass lasers—however, only at a very low repetition rate and hence low average power level [95–97]. High average powers ranging from tens to hundreds of watts recently became available from diode-pumped fiber, slab, and cryogenically cooled thick-disk lasers [98–109]. Because of excessive accumulation of nonlinearly induced phase shifts in their long gain media, their scaling to much higher energies requires large-aperture (meter-scale) and hence extremely

Table 1. Performance of Yb-Doped Few-Picosecond High Average and High Peak Power Systems[a]

P_{peak}	P_{avg}	E_{pulse}/τ_{pulse}	f_{rep}	Reference
		Fiber laser systems		
12 MW	830 W	10.6 μJ/640 fs	78 MHz	[100]
0.75 GW	93 W	93 μJ/81 fs	1 MHz	[102]
1.8 GW	530 W	1.3 mJ/670 fs	400 kHz	[106]
		Slab laser systems		
37 MW[b]	140 W	43 μJ/1.1 ps	3.25 MHz	[108]
80 MW	1.1 kW	55 μJ/615 fs	20 MHz	[99]
23 GW[b]	250 W	20 mJ/830 fs	12.5 kHz	[110]
		Cryogenically cooled laser systems		
0.65 MW[b]	430 W	8.6 μJ/12.4 ps	50 MHz	[104]
8.7 MW[b]	93 W	93 μJ/10 ps	1 MHz	[105]
73 MW	19.4 W	1 mJ/11.7 ps	20 kHz	[98]
7 GW[b]	60 W	12 mJ/1.6 ps	5 kHz	[103]
2 GW[b]	64 W	32 mJ/15 ps	2 kHz	[101]
170 GW	100 W	1 J/5.1 ps	100 Hz	[109]
		Thin-disk laser systems		
1.4 GW[b]	200 W	2 mJ/1.3 ps	100 kHz	[206]
17.6 GW[b]	300 W	30 mJ/1.6 ps	10 kHz	[147]
38.8 GW[b]	200 W	40 mJ/0.97 ps	5 kHz	Fig. 5(b)
27.6 GW[b]	100 W	50 mJ/1.7 ps	2 kHz	[134]
—	—	200 mJ	5 kHz	under development
—	—	2 J	10 kHz	envisioned

[a]Peak power (P_{peak}), average power (P_{avg}), pulse energy (E_{pulse}), pulse duration (τ_{pulse}), and repetition rate (f_{rep}) of selected Yb:YAG fiber, slab, cryogenically cooled, and thin-disk amplifier systems delivering pulses with a duration of a few picoseconds or shorter. The data are taken from the corresponding references.

[b]Peak powers have been calculated assuming a Gaussian pulse shape ($P_{peak} \approx 0.94 * E_{pulse}/\tau_{pulse}$).

expensive diffraction gratings for implementing CPA [102,106,110] or complex architectures, such as the coherent combination of a large number of parallel beams [111], or possibly coherent pulse stacking [112]. Diode-pumped ytterbium-doped thin-disk lasers offer energy and peak-power scalability from simple, cost-effective assemblies. Therefore, in what follows we focus on this technology as a promising candidate for driving broadband OPA systems scalable to high average and peak powers. Nevertheless, we stress that diode-pumped fiber, cryogenically cooled thick-disk, and slab lasers constitute a highly competitive alternative at high repetition rates and moderate peak power levels, and we kindly refer the reader to recent reviews of these approaches [33,107,113–116]. Table 1 summarizes the parameters of some of the best-performing systems based on Yb-doped fiber, slab, cryogenically cooled thick-disk, and thin-disk technology.

A. Toward High Peak and Average Powers

Ever since its first demonstration in 1994 [117], the thin-disk laser has been one of the most promising concepts for scaling sub-picosecond pulses to the highest peak and average powers. In this section we briefly summarize the basic features of thin-disk technology and refer the reader to Supplement 1 and recent reviews [118–120] for a more detailed discussion of performance, limitations and ways of overcoming them.

In a thin-disk laser the active medium is a thin and relatively large-diameter disk, typically tens to hundreds of micrometers in thickness and few (tens) millimeters in diameter. Crystals are used due to their favorable thermal and mechanical properties compared to glasses, with ytterbium-doped yttrium aluminium garnet (Yb:YAG) being the paradigm material of choice to date, although thin-disk lasers using different disk materials such as Yb:Lu_2O_3 [121,122], Yb:CALGO [123], and ceramic Yb:YAG disks [124,125] have also been demonstrated.

A Yb:YAG laser disk is coated on the back side to act as a high-reflective (HR) mirror for both the pump and the laser wavelengths. The other (front) side is antireflection (AR) coated for both wavelengths [see Fig. 3(a)]. The HR-coated side of the disk is firmly fixed onto a supporting substrate, which, in turn, is mounted on a water-cooled assembly. To achieve good (90% or more) absorption of the pump light, the pump beam is delivered at an angle from the front side and reflected in a number of passes using a special imaging multipass assembly [Fig. 3(b)]. Heat removal from the crystal is realized along the optical axis of the resonator. This minimizes thermally induced changes in the optical properties of the laser medium across the laser beam and allows for extremely high pump power densities reaching and exceeding 10 kW/cm^2 [118,126,127]. Energy and power scaling can be accomplished by scaling the diameter of the disk along with the pump and laser beams, which is eventually limited by amplified spontaneous emission (ASE) [128,129].

The small length of the gain medium greatly suppresses nonlinear focusing during the amplification of ultrashort pulses as compared to other laser geometries. As a result, CPA can be implemented with substantially smaller temporal stretching, requiring smaller, less expensive diffraction gratings as compared to other solid-state ultrashort pulse amplifiers [99,107]. These superior features of the thin-disk laser geometry come at the expense of a low single-pass gain of typically 10%–15% (small signal). This shortcoming can be mitigated by multiple passages and/or the serial combination of several disks [118,130,131].

Thin-disk gain modules have been used for ultrashort pulse generation in mode-locked oscillators [132,133] and regenerative [134] and multipass [135] amplifiers. Thousands of them have been tried and tested in 24/7 service for industry. This mature technology constitutes an ideal basis for scaling subpicosecond pulses to unprecedented combinations of peak

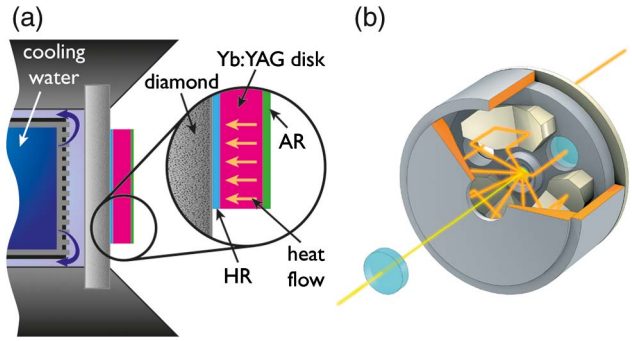

Fig. 3. Schematics of thin-disk laser technology. (a) Cold finger with substrate showing the cooling mechanism in a disk laser head, (b) disk laser head showing the principle of the pump light reimaging technique onto the thin-disk active medium (courtesy of TRUMPF Laser GmbH).

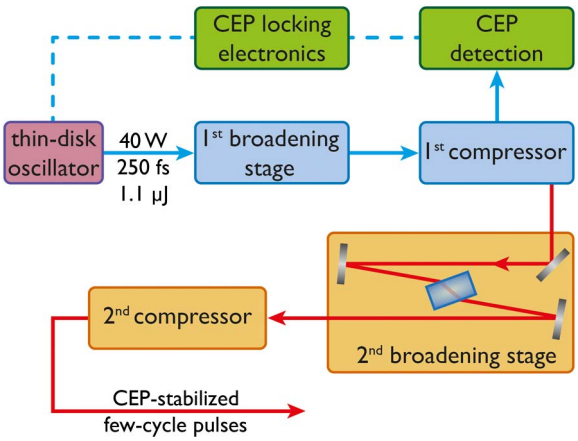

Fig. 4. Schematic of a KLM Yb:YAG laser system. Pulses from the oscillator centered at 1030 nm with an energy of 1.1 μJ and a duration of 250 fs at a repetition rate of 38 MHz are passed through a two-stage compressor made up of a solid-core large-mode-area fiber (first broadening stage), a bulk crystal as the nonlinear media (second broadening stage), and chirped mirrors forming the dispersive delay lines (first and second compressors), resulting in carrier-envelope-phase (CEP)-stabilized few-cycle output pulses [144].

and average power levels for driving OPAs in 3FST [136]. The remaining part of this section reveals how this technology can provide both the broadband seed and the high-power pump pulses in a perfectly synchronized fashion to this end.

B. Mode-Locked Ytterbium-Doped Thin-Disk Oscillators

Ultrashort pulse generation from a diode-pumped Yb-doped thin-disk laser oscillator was first demonstrated by Keller and co-workers at the turn of the millennium [137]. The technology was subsequently advanced to average power levels of hundreds of watts [138], pulse energies of several microjoules [130,139,140], and pulse durations shorter than 100 fs [131,141] directly from the oscillator. Kerr-lens mode locking (KLM) [49] and semiconductor saturable absorber mirrors [142] have been the methods of choice for mode locking [137,143].

Figure 4 shows the schematic of a KLM Yb:YAG thin-disk-oscillator-based few-cycle source [144]. The system delivers reproducible waveform-controlled few-cycle pulses at an average power exceeding that of few-cycle Ti:Sa oscillators by more than an order of magnitude.

The average power of KLM Yb:YAG thin-disk oscillators was recently increased by nearly an order of magnitude to deliver 14 μJ, 330 fs pulses at a 19 MHz repetition rate [140]. These advances open up the prospect of a megahertz source of near-infrared (NIR) femtosecond continua with a peak power of several hundred megawatts at average power levels of the order of 100 W and, if needed, with a controlled waveform. Such a source holds promise for greatly expanding the range of applications of ultrashort pulsed laser oscillators (as a stand-alone system) and for serving as a front end for gigawatt-to-terawatt 3FST architectures (see Fig. 2 and discussion in Section 3).

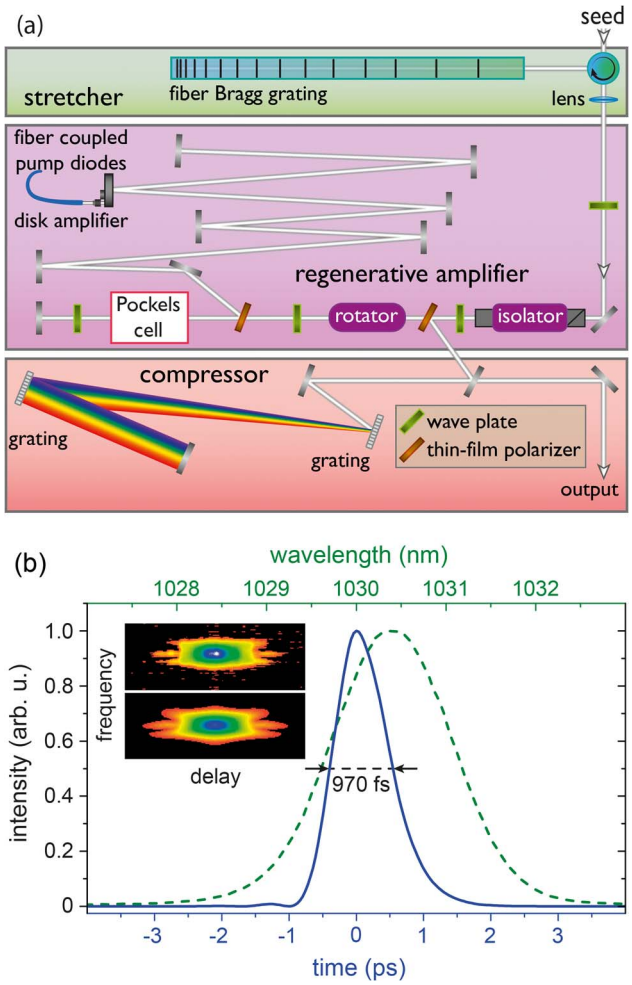

Fig. 5. Thin-disk regenerative amplifier. (a) Typical schematic layout. The subpicosecond seed pulse is temporally stretched before entering the thin-disk Yb:YAG regenerative amplifier. The amplified pulses are recompressed in a grating compressor. (b) Measured spectrum (green dashed line) and temporal intensity profile (blue line) from a system equipped with two disk modules (disk parameters: doping concentration >7%, thickness ~100 μm, beveled and roughened edge, TRUMPF Laser GmbH). These 0.97 ps pulses carry an energy of 40 mJ at a repetition rate of 5 kHz, corresponding to an average power of 200 W. The corresponding measured (top) and reconstructed (bottom) FROG traces are shown as insets (G error: 0.0024).

C. Thin-Disk Regenerative Amplifiers for Pumping OPCPA

The first thin-disk-based regenerative amplifier was demonstrated in 1997 and generated 2.3 ps pulses with energies up to 0.18 mJ and an average power of the order of 1 W [145]. A decade of development work advanced the technology into the multimillijoule, tens of watts regime [146]. By drawing on commercial Yb:YAG thin-disk modules originally designed for multikilowatt-class cw products, continued efforts led to near-1-ps pulses with energies as high as 30 mJ and average powers reaching 300 W at repetition rate of 10 kHz [147]. Milestones of this evolution are listed in Table 1, and a schematic of the architecture of state-of-the-art systems is shown in Fig. 5(a). All results on picosecond CPA with thin-disk lasers

referred to or reported directly in this work have so far been achieved with standard Yb:YAG thin-disk laser modules designed and fabricated for industrial lasers. This suggests that there may be some room left for further optimization of thin-disk Yb:YAG chirped-pulse amplifiers.

Thanks to their superior thermal management and low B integral, Yb:YAG thin-disk regenerative amplifiers deliver their near-bandwidth-limited pulses in a near-diffraction-limited beam ($M^2 < 1.1$) with excellent pulse-energy stability characterized by a drift smaller than 1% over 12 h. Figure 5(b) presents the measured optical spectrum and the retrieved temporal profile showing a full width at half-maximum (FWHM) pulse duration of 0.97 ps of an Yb:YAG thin-disk regenerative amplifier composed of two thin-disk amplifying modules within one resonator, delivering 40 mJ pulses at a repetition rate of 5 kHz.

While 40 mJ at 200 W and 30 mJ at 300 W [147] represent current records in high-energy 1-ps-scale pulse generation with high average power, none of these values individually appear to even come close to the ultimate limits of picosecond thin-disk laser technology. In fact, a regenerative amplifier followed by a multipass amplifier recently boosted the energy of sub-2-ps pulses to more than 500 mJ at a repetition rate of 100 Hz [148]. At a much higher repetition rate (800 kHz), 7 ps pulses from a commercial thin-disk laser were amplified to an average power of 1.1 kW [135]. An amplifier chain containing two thin-disk-based multipass amplifiers as final stages delivers 14 kW, 140 mJ in a 10 Hz burst mode [149].

Thanks to their optimum pulse duration of the order of 1 ps and excellent beam quality, thin-disk Yb:YAG regenerative amplifiers allow for efficient generation of second-harmonic and third-harmonic light by $\chi^{(2)}$ processes [second-harmonic generation (SHG) and sum-frequency generation (SFG), respectively]. As an example, results achieved with 1.3 ps, 1030 nm pulses from a multikilohertz Yb:YAG thin-disk laser demonstrate a second-harmonic conversion efficiency as high as 74% in a 1.5 mm thick LiB_3O_5 (LBO) crystal ($\theta = 90°$, $\varphi = 12.9°$).

OPA relies on a spatial as well as temporal overlap of the pump and seed pulses for efficient amplification. Hence, pump and seed pulses are derived from the same femtosecond laser [136,150] serving as the common front end. However, the pump pulse suffers a delay of several microseconds upon passage through the regenerative and/or multipass amplifier(s). This delay is compensated for by selecting a correspondingly delayed seed pulse from the train delivered by the common front end. Already fractional changes as small as 10^{-7} 10^{-8} (by air turbulences, mechanical vibrations, and expansion due to temperature drifts) in the microsecond delay of the pump and seed pulses suffered upon passage through different optical systems may cause an excessive timing jitter [151] and require active stabilization.

Spectrally resolved cross correlation of the seed and the pump pulses offers a powerful means of active synchronization [152]. A possible implementation of this concept is based on stretching a small fraction of the broadband seed pulse to a duration of several picoseconds and mixing this pulse with the narrowband pump pulse in a nonlinear crystal. Changes in the carrier wavelength of the resultant sum-frequency output are unambiguously related to the relative timing between pump and seed pulses. In its first demonstration, this stretched-pulse cross-correlation technique was capable of reducing the RMS timing jitter to $\sigma = 24$ fs over the frequency band of 20 mHz to 1.5 kHz [153].

Recently, this method was improved by replacing the sum-frequency generator by an OPA stage and deriving the timing information (optical error signal) from the spectrally resolved amplified signal output [154]. For this approach it is sufficient to split off only ~2 pJ of the seed pulse energy, since with the amplification of the seed pulse the OPA inherently delivers an amplified error signal. The concept is schematically depicted in Fig. 6(a). Its first implementation yielded pump–seed timing stabilization with a record residual RMS jitter of less than 2 fs over the frequency band ranging from 0.1 Hz to 1 kHz as well as long-term timing stability [Fig. 6(b)], ensuring ideal conditions for stable OPCPA operation.

D. Scaling Thin-Disk Amplifiers—Future Prospects

Present-day industrial thin-disk laser technology is capable of transforming diode-laser light of poor beam quality into kilowatts of power delivered in a diffraction-limited laser beam. The overriding question is to what extent this tremendous potential can be exploited for *simultaneously* boosting the energy *and* average power of near-1-ps laser pulses. Scaling of power and energy have already been demonstrated *separately*

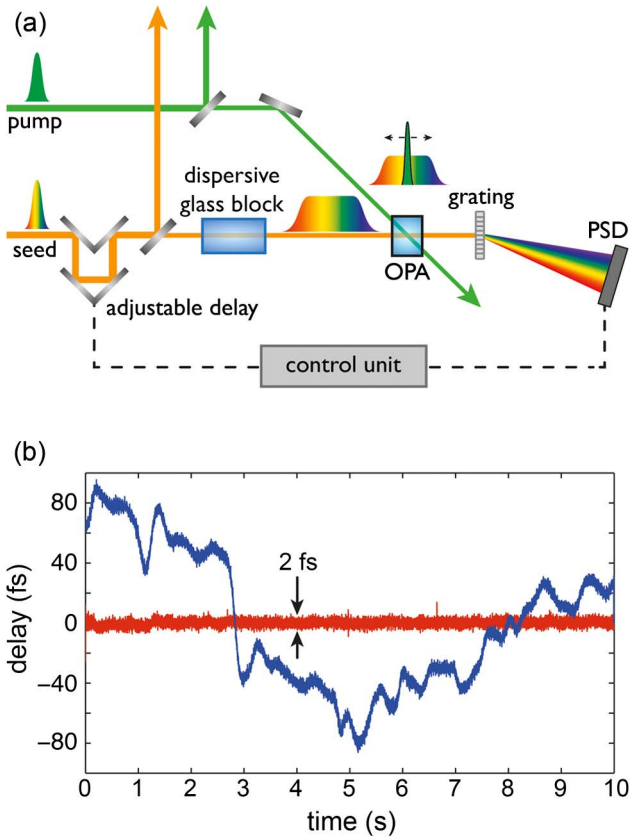

Fig. 6. Active pump-seed temporal synchronization system. (a) Schematic layout. PSD, position sensitive detector. (b) Timing fluctuations on the order of ±100 fs are reduced to a residual RMS jitter of less than 1.9 fs; for details, see [154].

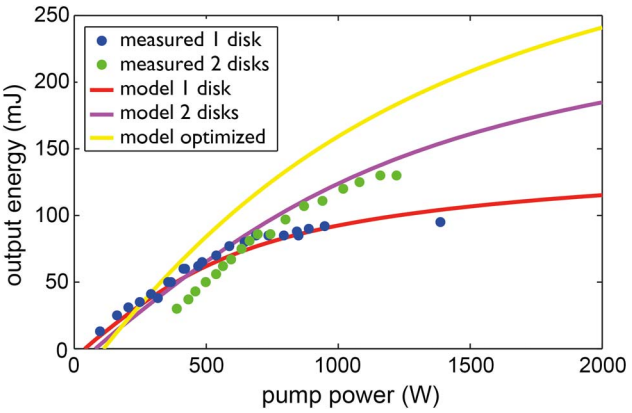

Fig. 7. Performance of cw diode-pumped regenerative amplifiers utilizing commercial thin-disk modules (disk parameters: doping concentration >9%, thickness ~120 μm, beveled and roughened edge, TRUMPF Laser GmbH). In a linear cavity setup, 95 mJ output energy was demonstrated at a 1 kHz repetition rate with one standard disk pumped at 940 nm (blue dots). While there were indications of energy saturation, the energy was boosted to 130 mJ by adding a second disk (green dots). By further optimization of both disk parameters and the pump design, more than 200 mJ energy at 5 kHz can be achieved (yellow line).

beyond 1 kW [135] and up to 1 J [155–157], respectively. Achieving these values of both energy and average power in the same thin-disk laser system will require optimal scaling of the disk diameter (increasing the available energy but also the depopulation losses) and disk thickness (increasing the available energy and the deleterious thermal effects) [118].

A regenerative amplifier equipped with commercial Yb:YAG thin-disk modules is being developed in our laboratory for generating 200 mJ pulses at a 5 kHz repetition rate. In preliminary experiments with a linear cavity amplifier, 95 and 130 mJ pulses at a repetition rate of 1 kHz have been demonstrated, with one and two disk modules, respectively (Fig. 7), with the latter being limited by thermal effects in the Faraday isolator preventing feedback into the front end [158]. The use of a ring cavity will remove this limitation and—based on these preliminary results—holds promise for achieving the above target parameters. A rate-equation model of thin-disk laser energy that takes into account the decrease in the upper level lifetime, caused by ASE [120] and the disk temperature, shows good agreement with the measurements and indicates that the same energy can be extracted up to 5 kHz with the current disks. An optimized design with increased disk thickness pumped at 969 nm can further increase the extracted energy, using the same beam size of 5 mm.

Much higher energies and powers can be expected from larger apertures [159]. The feasibility of scaling near-1-ps thin-disk amplifiers to the 1 J frontier was recently demonstrated [155–157]. Further discussion on how careful engineering of large-aperture Yb:YAG disk amplifier modules for minimizing ASE and temperature control could permit scaling of the amplified energy to the joule-kilowatt level is given in Supplement 1.

Such large-aperture Yb:YAG disks have been shown to be capable of handling more than 10 kW of diode laser power [160]. Merely a couple of thin-disk amplifier modules equipped with 20-mm-diameter Yb:YAG disks and pumped by approximately 30 kW of cw diode laser light each will be sufficient to boost the energy of the 0.2 J seed pulses—delivered by two 5 kHz regenerative amplifiers in a parallel architecture—to the level of 2 J at a 10 kHz repetition rate. A possible approach to this goal is schematically illustrated in Fig. 8. Should scaling to this energy level encounter unexpected difficulties, coherent combination of several amplifiers [25,161–163] or the concept of pulse stacking [112] might provide a remedy. These developments may open the door for a kilowatt-class 3FST source of few-cycle or tunable multiterawatt femtosecond pulses.

3. BROADBAND OPCPA PUMPED BY NEAR-1-PS PULSES

With robust nonlinear crystals and a reliable, cost-effective, and power-scalable short-pulsed pump-laser technology along with methods for accurate pump-seed timing synchronization in place (see Section 2.C), near-1-ps-pulse-pumped OPCPA offers several advantages over *both* long-pulse-driven OPCPA *and* conventional CPA implemented in solid-state laser amplifiers. First, the amplifier crystals can be pumped at much higher intensities [27–29], allowing high gains to be realized with very thin crystals, i.e., in combination with broad amplification bandwidths. Second, the short pump window also greatly simplifies the implementation of CPA and dispersion control and, finally and most importantly, improves the temporal contrast of the amplified signal dramatically on the nanosecond to few-picosecond time scale.

The gain bandwidth can be even further extended, up to several octaves, by using different crystals or crystals with different orientations yielding shifted gain bands and utilizing multiple pump beams [164] at all wavelengths where they can be made available with good wall-plug efficiency, i.e., at 1030 nm and its low-order harmonics at 515 and 343 nm. This constitutes the basis for developing the prototypical broadband or broadly tunable sources of 3FST. The very same front end and multicolor pump source may be utilized for both purposes. In what follows, we shall discuss the feasibility of these 3FST sources and their expected performance when being pumped with several-kilohertz, kilowatt-class thin-disk lasers recently demonstrated [147] and systems that are currently under development [158].

A. Basic Theory

In the OPA process, energy is transferred from a high-frequency, high-intensity (pump) beam to a low-frequency, low-intensity (seed or signal) beam in a birefringent [165] nonlinear crystal, while a third beam, the idler, is generated. By polarizing the pump along the fast axis and the signal or idler or both along the slow axis, conservation of energy and momentum of the participating (pump, signal, idler, labeled with p, s, and i, respectively) photons can be simultaneously fulfilled:

$$\hbar\omega_p - \hbar\omega_s - \hbar\omega_i = 0, \tag{1}$$

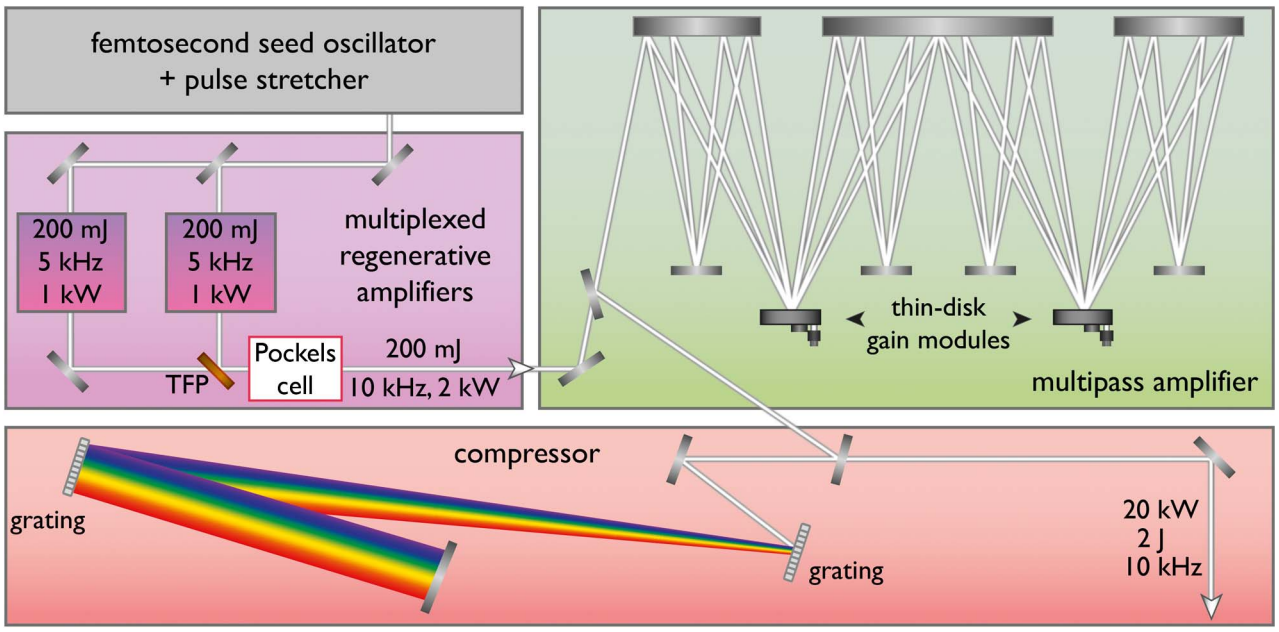

Fig. 8. Schematic layout of the multikilowatt, joule-class picosecond laser setup. A regenerative amplifier and a subsequent multipass amplification stage are used for generating multikilowatt, joule-class picosecond pulses (TFP, thin-film polarizer). Pulses from a front end comprising an oscillator and a pulse stretcher (cf. Fig. 5) are used to seed two regenerative amplifiers working at a 5 kHz repetition rate. The 200 mJ amplified pulses from both amplifiers are interleaved in time to produce a 10 kHz, 200 mJ pulse train. These pulses are then guided to a multipass amplifier using two thin-disk laser heads. Finally, the amplified pulses are compressed in a grating compressor.

$$\vec{k}_p - \vec{k}_s - \vec{k}_i = 0. \tag{2}$$

In the classical description of the process, Eqs. (1) and (2) account for the parametric frequency downconversion and phase (velocity) matching of the participating waves, respectively. Due to dispersion, these conditions can be fulfilled over a limited range of signal frequencies only, which manifests itself in a finite parametric gain bandwidth $\Delta\nu$ [166,167]:

$$\Delta\nu = \frac{2(\ln 2)^{1/2}}{\pi}\left(\frac{\Gamma}{L}\right)^{1/2}\left|\frac{1}{v_{gi}} - \frac{1}{v_{gs}}\right|^{-1}, \tag{3}$$

where L is the length of the nonlinear medium, Γ is the parametric gain coefficient proportional to the pump-field amplitude and the effective nonlinear optical coefficient, and $\nu_{gi,s}$ stand for the group velocity of the idler and the signal, respectively [166]. Equation (3) suggests that temporal walk-off between the amplified pulses limits the achievable gain bandwidth.

In sharp contrast with lasers, the central frequency and the width of the OPA gain band can be manipulated by changing the orientation or temperature of the crystal, and/or by the pump-signal propagation geometry. These degrees of freedom can be used to produce tunable femtosecond pulses. Alternatively, degenerate OPA near the wavelength where the group-velocity dispersion for the signal and idler beams becomes zero ($\omega_s \simeq \omega_i \simeq \omega_p/2$) [167] or the noncollinear OPA [77,78,168–170] permits the amplification of few-cycle pulses [171,172]. Both modes of operation can be simultaneously implemented in several OPA channels driven by the third or second harmonic or the fundamental of the 1030 nm picosecond pulses from Yb:YAG thin-disk amplifiers to yield synchronized tunable or few-cycle pulses in the visible (VIS), NIR, and mid-infrared (MIR) spectral ranges, respectively. These pulses may also be superimposed on each other for the synthesis of multi-octave light transients [173–175]. These options call for a seed coming in the form of a coherent, phase-stable, multi-octave supercontinuum covering the entire wavelength range of interest.

B. Generation of Waveform-Controlled Continua for OPA Seeding

The NIR continuum produced by the prototypical carrier-envelope-phase (CEP)-stabilized femtosecond KLM thin-disk-laser-based source described in Section 2.B [144], constitutes—after proper active synchronization to the pump pulses (see Section 2.C)—an ideal seed for broadband OPA. In fact, these CEP-stabilized continua exhibit a well-behaved spectral phase and excellent spatial beam quality and are delivered with microjoule-scale energy, allowing efficient OPA with low fluorescence background. The spectrum is perfectly matched to the gain band of BBO and LBO parametric amplifiers [136] pumped by the second harmonic of the Yb:YAG laser (515 nm).

Amplification in such an OPA to the millijoule energy level and recompression of the amplified NIR pulse may be followed by further spectral broadening in a gas-filled hollow-core fiber (HCF). Self-phase modulation and self-steepening broadens the input spectrum predominantly toward shorter

wavelengths. This approach can provide the broadband seed required by a VIS-OPCPA pumped by the third harmonic of the Yb:YAG laser (343 nm) but fails to do so for a MIR-OPCPA driven directly at 1030 nm. In the remaining part of this section we discuss the generation of a phase-stable continuum in the MIR and its subsequent extension to shorter wavelengths.

A powerful technique for the generation of CEP-stabilized MIR continua has been difference frequency generation (DFG) [176,177]. This process creates a CEP-stable output from a non-CEP-stabilized femtosecond pulse and has been successfully applied to seeding few-cycle MIR-OPA systems [166,178,179]. The output of the sub-10-fs NIR source described in Section 2.B can—after preamplification in a single broadband OPA stage pumped at 1030 nm—efficiently drive DFG to yield a continuum in the 1.5–2.5 μm range [180]. The oscillator does not need to be CEP stabilized, since the CEP of the fundamental cancels out in the DFG process.

The spectrum of the DFG output can be efficiently extended in a gas-filled HCF [181] to cover the multi-octave range of 400–2500 nm. The main building blocks of such a supercontinuum generator are sketched in Fig. 9(a). The 10-fs-scale seed pulses may possibly also be derived directly from the output of the near-1-ps Yb:YAG pump source by cascaded temporal compression [182], as indicated by a dashed line in Fig. 9(a). This approach would greatly relax the need for the active pump-seed synchronization system for the OPCPA described in Section 2.C, because both the pump and the seed would travel comparable optical paths.

All essential processes underlying the above concept have already been successfully demonstrated. In fact, we have recently generated IR continua [shown in Fig. 9(b)] from few-cycle NIR pulses with an efficiency exceeding 10% [180]. Moreover, the spectrum from a MIR-OPA seeded by a similar CEP-stable continuum could be efficiently broadened in a gas-filled HCF to cover the entire VIS-NIR-MIR spectral range of 400–2500 nm, which is also shown in Fig. 9(b). The temporal characterization of the continuum by second-harmonic frequency-resolved optical gating (FROG) shows the high degree of coherence and compressibility of the generated multi-octave spectrum in Fig. 9(b) [183]. This indicates such continua, at energy levels of hundreds of microjoules, are achievable with few-cycle MIR pulses, in agreement with theoretical predictions [181]. The seed signals for the simulated OPCPA systems discussed below are derived from the multi-octave continuum shown in Fig. 9(b).

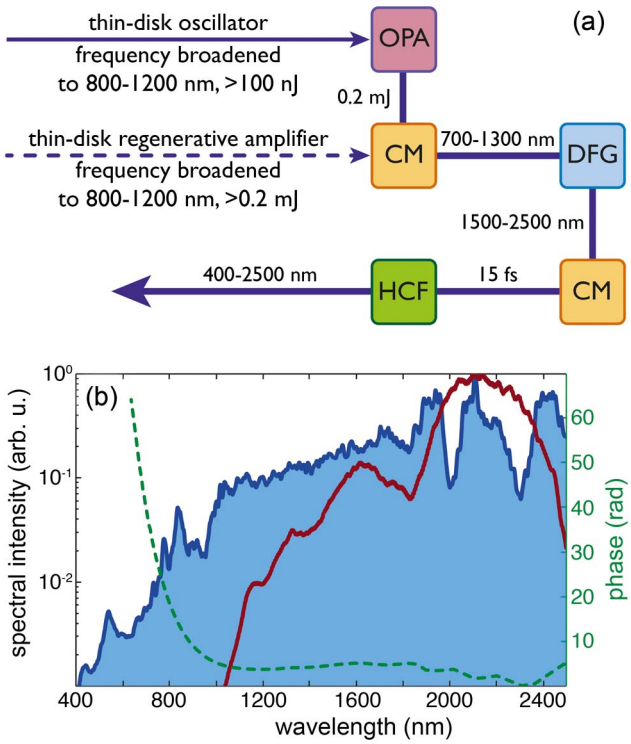

Fig. 9. Multi-octave seed generation. (a) Near-three-octave seed generation schemes based on the output from the oscillator described in Section 2.B or driven by the amplified subpicosecond pulse characterized in Fig. 5(b) (dashed arrow). The spectrally broadened and compressed output of the Yb:YAG oscillator is amplified in an OPA stage to 50 μJ of energy and subsequently compressed in a chirped-mirror compressor (CM) to about 6 fs for efficient difference frequency generation (DFG). The resultant broadband DFG signal, centered at about 2 μm, is compressed and focused into a gas-filled hollow-core fiber to extend the spectrum into the visible range. This approach provides a near-three-octave, phase-stable continuum at the energy level of the order of 1 μJ. Alternatively, spectrally broadened subpicosecond millijoule-scale pulses directly from the amplifier circumvent the need for an additional OPA stage and may result in a phase-stable supercontinuum at the level of several hundred microjoules. (b) Broadband phase-stable continua generated in preliminary experiments. Red curve: Difference-frequency radiation in a 500-μm-thick type-I BBO crystal optimized for 12% conversion efficiency. Blue shaded area: Spectral broadening of a parametrically amplified three-cycle DFG signal in a gas-filled hollow-core fiber to a supercontinuum containing 330 μJ of energy. The detected bandwidth of the spectrum in both cases is limited by the sensitivity of the spectrometer in the IR tail. The dashed green curve shows the measured spectral phase of the generated supercontinuum using the FROG technique. The red curve in (b) is reproduced from [180].

C. Prototypical OPCPA Architectures in 3FST

The common backbone for all prototypical 3FST architectures we propose and numerically analyze in the following sections consists of (i) a high-power femtosecond laser, in our case a 100-W-scale KLM Yb:YAG thin-disk oscillator, followed by (ii) the multi-octave seed generation described in the previous section and (iii) a multi-100-W-to-kW-scale source of multi-mJ, near-1-ps-pulses, in our case based on Yb:YAG thin-disk amplifiers, see Fig. 10(a). The supercontinuum seed [see Fig. 10(a)] is split into three spectral channels: VIS centered at 550 nm, NIR centered at 1 μm, and MIR centered at 2 μm, by using chirped dichroic beam splitters [173,184,185].

Each of the three OPA channels can be used to generate tunable multi-cycle pulses which will be described in Section 3.D or to yield few-cycle pulses as will be shown in Section 3.E. Their pump pulses are generated by a simple frequency-converter module comprising two LBO crystals. Our crystal of choice is LBO instead of BBO, owing to its availability in large sizes and its small spatial and temporal

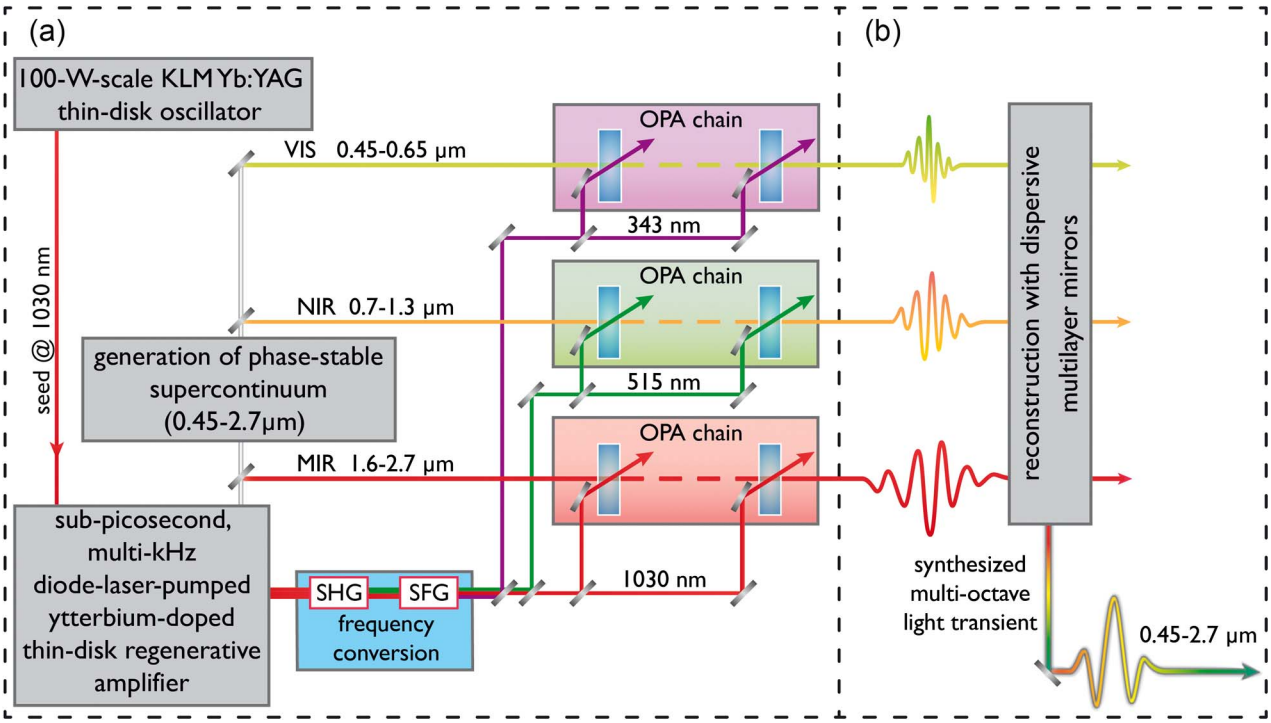

Fig. 10. Prototypical multi-octave 3FST field synthesizer (Section 3.E and Section 3.F). (a) Schematic architecture of a three-channel OPCPA system seeded and pumped by subpicosecond ytterbium lasers. A part of its output is used for generating the multi-octave supercontinuum signal, which is split into three channels, centered at 550 nm and 1 and 2 μm, respectively. The different channels are pumped by different (low-order) harmonics of the multimillijoule-level, kilohertz Yb:YAG regenerative amplifier output. Each channel supports few-cycle pulses after compression. Alternatively, using a similar concept, several-tens-of-femtoseconds multicycle pulses widely tunable from the UV to the IR spectral range can be produced. (b) By coherently combining the three few-cycle channels amplified in (a), nonsinusoidal multi-octave light transients can be generated.

walk-off, in spite of its smaller effective nonlinear coefficient. Second-harmonic generation (SHG) in the first one yields twin pulses of comparable energy at 515 nm and 1030 nm, which are mixed in the second crystal to produce a third pump pulse at 343 nm by sum-frequency generation (SFG). Moderate SHG and SFG conversion efficiencies (of about 50% and 20%–30%, respectively) ensure that all beams exiting the frequency converter unit have a good beam quality, which is important for OPCPA pumping. The three beams are subsequently separated by dichroic beam splitters and directed into the three OPA channels described in the following sections.

D. Power of 3FST: Tunability over Several Octaves

Time-resolved spectroscopy often requires tunable multicycle femtosecond pulses. The three OPCPA channels depicted in Fig. 10(a) can be designed to deliver wavelength-tunable femtosecond pulses. Their seed can be generated as described in the preceding section. We propose to produce the primary pump pulses at 1030 nm with the Yb:YAG thin-disk regenerative amplifier recently demonstrated, yielding 30 mJ, 1.6 ps pulses at a 10 kHz repetition rate, i.e., an average power level of 300 W [147]. The frequency converter described in the previous section distributes this pump energy among the three OPCPA channels. The super-continuum is divided into three bands centered at carrier wavelengths of 550 nm and 1 and 2 μm. They are seeded into the VIS, NIR, and MIR arms of the OPCPA system, each of which consists of two amplifier stages, using thin BBO, LBO, and $LiNbO_3$ crystals, pumped at 343, 515, and 1030 nm, respectively. For more details, see Supplement 1.

Pulse duration control and wavelength tuning of the amplified pulses is accomplished by temporally stretching the seed continua and controlling their delay with respect to the pump pulses. In fact, the pump temporal window of $\tau_{\text{pump}} \simeq 1$ ps slices out a fraction, $\Delta\nu_{\text{signal}}$, of the bandwidth of the (stretched) seed continuum, $\Delta\nu_{\text{seed}}$, which is inversely proportional to the duration τ_{seed} of the stretched seed: $\Delta\nu_{\text{signal}} \approx \Delta\nu_{\text{seed}}(\tau_{\text{pump}}/\tau_{\text{seed}})$ [see Fig. 11(a)]. Thanks to a near-linear chirp carried by the stretched seed, the carrier frequency of the amplified signal can be tuned by varying the delay of the seed with respect to the pump pulse and by setting the phase-matching angle of the amplifier crystal. Figure 11(b) shows a series of amplified signal spectra from simulations in the three channels pumped with pulses of a duration of $\tau_{\text{pump}} \simeq 1.7$ ps. The continua stretched to $\tau_{\text{seed}} \simeq 30$ ps yield—after recompression—sub-40-fs pulses tunable over several octaves from the VIS to the MIR spectral range. Synchronized femtosecond pulses with adjustable pulse duration and tunable carrier frequency at such a variety of wavelengths and unprecedented average power levels may open new prospects for sophisticated multidimensional spectroscopies and pump-control-probe schemes.

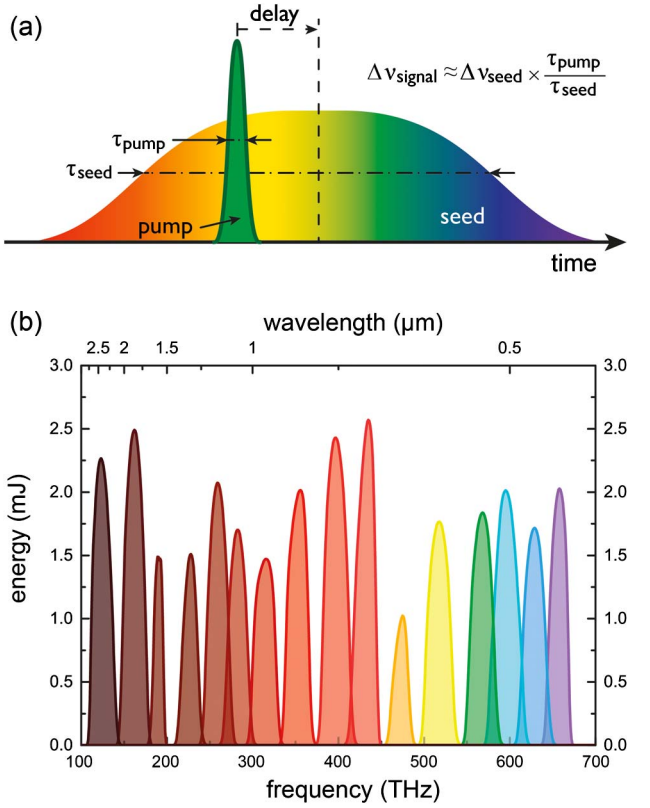

Fig. 11. Generation of widely tunable femtosecond pulses (Section 3.D). (a) Scheme for generating spectrally and temporally tunable pulses at any wavelength. The seed pulses are stretched to a significantly longer duration than that of the pump pulse. Amplification in a simple OPCPA setup yields pulses that can be spectrally tuned by changing the temporal delay between pump and seed pulses. (b) Amplified spectra of a widely tunable two-stage OPCPA system obtained from simulations. Millijoule-level, sub-40-fs pulses, tunable from 445 to 2750 nm, can be generated by using different harmonics of a 10 kHz Yb:YAG regenerative amplifier (see Supplement 1).

E. Power of 3FST: Multiterawatt VIS, NIR, and MIR Few-Cycle Waveforms

As an alternative to delivering tunable multicycle pulses, the three OPCPA channels of our prototypical 3FST system can be designed to generate few-cycle pulses at a single carrier wavelength from each channel, by broadband amplification and subsequent recompression of the continua seeded into the amplifier chains. Typical application fields of few-cycle pulses are attosecond science and extreme nonlinear optics, benefiting from peak powers as high as possible. Few-cycle pulses with multiterawatt peak powers are expected to allow scaling of the flux and/or the photon energy of attosecond pulses by increasing the beam size in high-harmonic generation (HHG) from ionizing atoms [22] or exploiting relativistic interactions with high-density plasmas at the surfaces of solids [186–191]. Therefore, we perform the following model calculations for a prototypical multicolor, multiterawatt few-cycle 3FST system by assuming the availability of the most powerful 3FST driver currently under development: a near-1-ps, 200 mJ, 5 kHz Yb:YAG thin-disk regenerative amplifier [158].

In our numerical study, we distribute the pump energy among the three OPA chains in favor of the NIR and MIR channels. This strategy is motivated by numerous applications benefiting from longer wavelengths [192–194]. Frequency conversion to the low-order harmonics as described in Section 3.C yields approximately 40 mJ at 343 nm, 74 mJ at 515 nm, and 86 mJ at 1030 nm for pumping the VIS, NIR, and MIR channels of the OPCPA system, respectively.

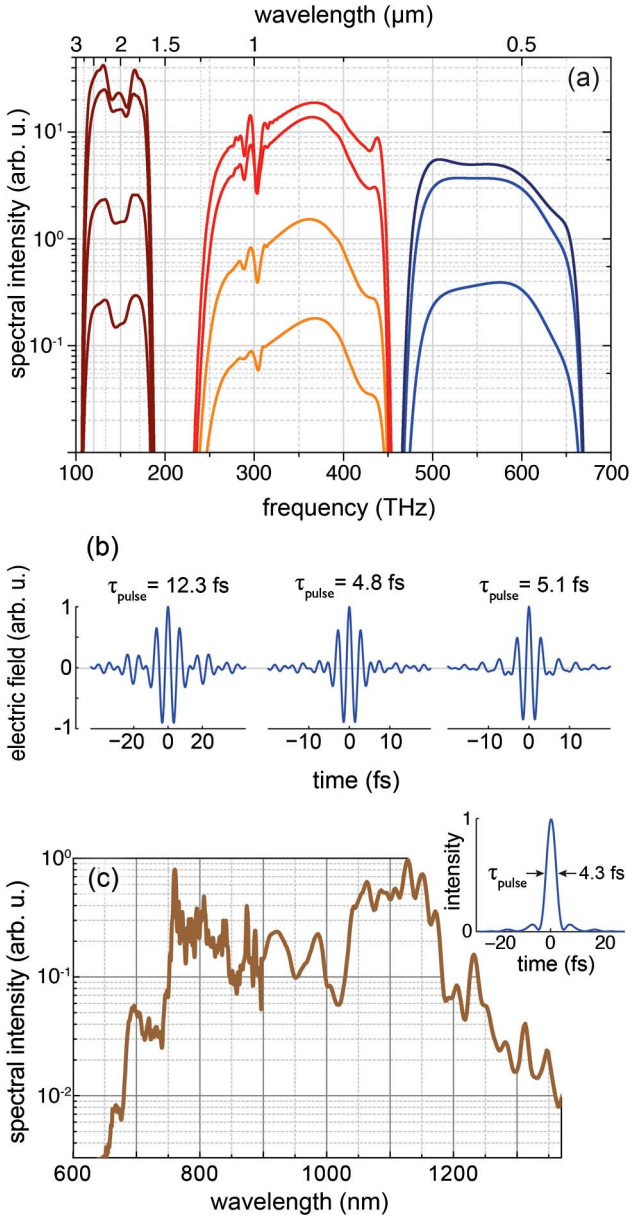

Fig. 12. Multi-octave amplified spectra of the three-channel synthesizer and corresponding waveforms (Section 3.E). (a) Spectra of the three-channel OPCPA synthesizer obtained from simulations. The spectra of the different stages in the different channels are normalized to their energy and shown on a logarithmic scale: VIS, blue; NIR, red-orange; IR, brown. For details of the simulations, see Supplement 1. (b) Fourier-transform-limited electric field associated with the output spectrum of each channel in (a); (c) amplified spectrum in a three-stage OPCPA chain. The spectrum contains 1.8 mJ and supports sub-5-fs pulses at a 3 kHz repetition rate.

The high intensity threshold for damage offered by the near-1-ps pump pulses allows a high single-pass gain in very thin (few-millimeter) OPA crystals, yielding a broad amplification bandwidth. The short length of the crystals is optimized for best gain saturation in each amplification stage. The energy is then boosted by using several amplification stages *without compromising the bandwidth.*

For the MIR channel using four $LiNbO_3$ crystals, our simulations predict an amplified pulse energy of 19.2 mJ, carried at a center wavelength of 2 μm, with a bandwidth-limited pulse duration of 12.3 fs (FWHM), corresponding to less than two cycles of the carrier wave. The pump-to-signal energy conversion efficiency in this channel is 22%, limited by back-conversion of the signal and idler into the pump via phase-matched SFG. In the NIR channel, 22.7 mJ pulses with a bandwidth-limited pulse duration of 4.8 fs can be expected (see Fig. 12), corresponding to a conversion efficiency of 30%. Thanks to the noncollinear geometry, parasitic back-conversion is strongly reduced, giving rise to an excellent efficiency. Last but not least, the VIS channel may yield 7.1 mJ pulses with a bandwidth-limited duration of 5.1 fs (Fig. 12). For details of the simulations, see Supplement 1.

In order to verify the credibility of this design study, we constructed a three-stage OPCPA test, seeded by a continuum derived from a Ti:sapphire front end (Femtopower Compact Pro Ti:sapphire multipass amplifier, Femtolasers GmbH) and pumped by an optically synchronized Yb:YAG thin-disk regenerative amplifier [136]. The 3 μJ seed pulse covering the spectral range of 500–1400 nm was generated in two stages of spectral broadening in a 120-μm-inner-diameter, 15-cm-long HCF filled with Kr atoms at a pressure of 5 bars and subsequently in a 2-mm-thick plate of YAG crystal using 30 μJ of the 1 mJ, 25 fs output pulses of the Ti:sapphire amplifier. The three subsequent stages of OPCPA used 2 mm LBO, 2 mm BBO, and 4 mm LBO as the nonlinear crystal, amplifying the spectral ranges of 800–1350, 670–1000, and 800–1350 nm, respectively. 1 mJ of a total energy of approximately 8 mJ of the 1.7 ps, 515 nm pump pulse drove the first stage, with the remaining energy and its fraction transmitted by the second stage pumping the second and third stages, respectively.

Figure 12(c) shows the spectrum of the amplified pulses supporting a transform-limited pulse duration of 4.3 fs (FWHM). The preliminary compression of the amplified spectrum to sub-10-fs pulses, utilizing a (not-yet-optimized) set of chirped mirrors, reveals a well-behaved spectral phase of the amplified signal, indicating its compressibility to the Fourier limit. The energy of the amplified pulses was 1.8 mJ, with negligible ASE content. The amplified bandwidth supporting sub-5-fs pulses and the conversion efficiency in excess of 20% achieved already in preliminary experiments create confidence in the predictions of our modeling.

F. Power of 3FST: Synthesis of Multi-Octave, Multiterawatt Light Transients

Waveform-controlled light transients with a bandwidth approaching two octaves have been demonstrated at microjoule energy and gigawatt peak power levels [173,184,195,196]. They allow temporal confinement of optical radiation to less than 1 femtosecond in subcycle waveforms [197,198]. With their power substantially enhanced, these extreme waveforms may open up a new chapter in nonlinear optics and attosecond science (thanks to, among other things, the feasibility of suppressing ionization up to unprecedented peak intensities and instantaneous ionization rates approaching optical frequencies, respectively). The prototypical three-color few-cycle OPCPA system described in the previous section offers a conceptually simple route to scaling multi-octave optical waveform synthesis to the multiterawatt regime.

To this end, the three channels delivering few-cycle pulses in the VIS, NIR, and MIR spectral ranges are recombined using a set of dichroic chirped mirrors to yield one beam in a scheme similar to that reported in [175,184]. Due to the difficulties of dispersion management, the high demands on a chirped-mirror compressor, and the required coating for the

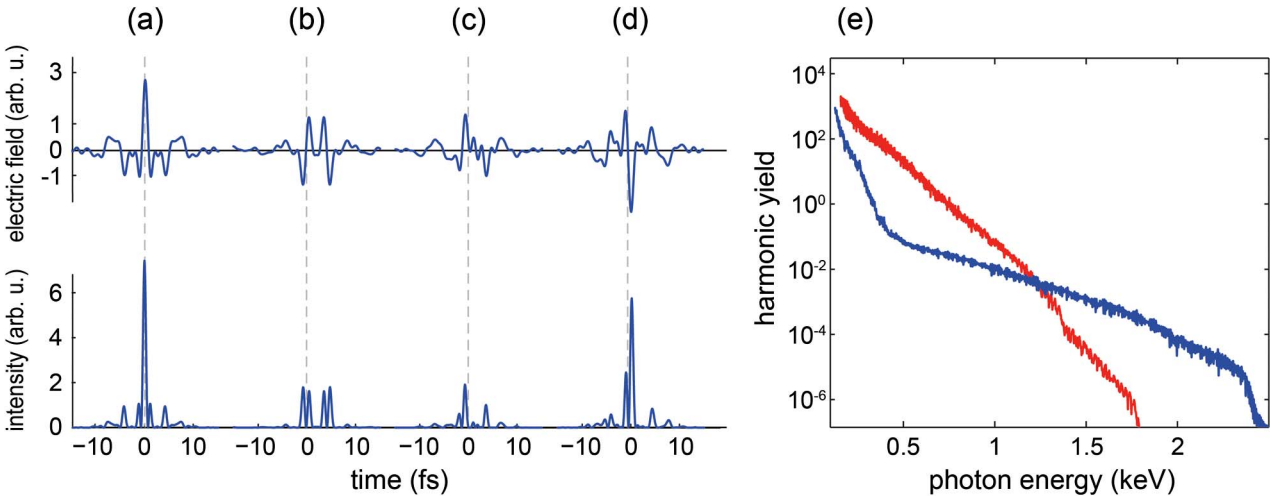

Fig. 13. Calculated synthesized waveforms from the three-channel OPCPA system and high-harmonic generation using synthesized waveforms (Section 3.E). (a) Fourier-transform-limited waveform; (b), (c) synthesized waveforms generated by changing the relative energy and time delay between different arms; (d) optimized waveform for HHG in terms of the highest cutoff energy of the synthesizer; (e) simulated HHG spectrum in helium. The red line represents the Gaussian-shaped pulse with 5 fs FWHM, whereas the blue line corresponds to the preoptimized waveform shown in (d).

OPCPA crystals in serial pulse synthesis [195], a parallel-synthesis [199] approach is chosen. Furthermore, fluctuations and drifts in the relative timing of the recombined pulses need to be suppressed to a tiny fraction of the half-field cycle for a stable waveform resulting from the coherent superposition [200]. This optical timing synchronization can be accomplished with the required sub-100-as precision with a balanced optical cross correlator demonstrated recently [175,196]. The feasibility of super-octave optical waveform synthesis was recently demonstrated in the NIR–VIS–UV spectral range by seeding a three-channel [184] and, more recently, four-channel [197] synthesizer consisting of broadband chirped mirrors with a continuum originating from a Ti:sapphire-laser-driven hollow-fiber/chirped-mirror compressor. Implementation with an OPA system is also being prepared [199,201,202].

Merely the adjustment of the relative timing of the three pulses emerging from the three OPA channels can result in a great variety of electric field forms on the time scale of the optical cycle. In fact, Figs. 13(a)–13(d) depict a few representative waveforms that may be synthesized from bandwidth-limited pulses emerging from the three channels described in the preceding section by varying their relative timing upon recombination. Further degrees of freedom for waveform sculpting can be introduced by shaping the amplitude and phase of the spectra of the individual channels, e.g., via an acousto-optic pulse shaper [203] and/or a spatial light modulator [204].

4. CONCLUSIONS AND OUTLOOK

Femtosecond technology emerged from nonlinear optical techniques allowing both the production and the characterization of femtosecond laser pulses. Its first generation (1FST) relied on dye lasers and delivered femtosecond pulses with peak and average powers up to the 100 MW and 100 mW ranges, respectively, over a narrow spectral range largely confined to 600–900 nm. Broadband solid-state laser media with high saturation fluence and CPA heralded the second generation of femtosecond technology (2FST), allowing for a boost of the peak and average powers of sub-100-fs pulses to the multiterawatt or 10 W regime, respectively, but not both of them simultaneously. Powerful 2FST systems are able to produce femtosecond pulses over an extended range of frequencies from the far-IR to the extreme UV via coherent frequency conversion based on $\chi^{(2)}$ and $\chi^{(3)}$ nonlinearities. However, these secondary sources are limited to power levels that are several orders of magnitude lower. The range of carrier wavelengths of powerful primary 2FST sources is—similar to 1FST—rather limited, currently spanning about 0.7–1.1 μm.

Based on OPCPA driven by terawatt-scale pulses from ytterbium lasers at kilowatt-scale average power (so far demonstrated with water-cooled thin-disk and slab and cryogenically cooled thick-disk technologies), third-generation technology (3FST) allows boosting the peak *and* average powers of coherent femtosecond light *simultaneously* to the multiterawatt and hundreds of watts range, respectively. It is capable of doing so over a wavelength range extended to more than two octaves, spanning 0.45–2.5 μm with either

(i) tunable, synchronized, multicycle, VIS, NIR, MIR tens of femtoseconds duration pulses,
(ii) synchronized, few-cycle VIS, NIR, MIR few-femtosecond-duration pulses, or
(iii) subcycle to few-cycle light transients synthesized from all spectral components,

available within the above multi-octave region, in all cases with full control over the generated light waves. These operation modes are being offered by a single basic system architecture and basic instrumentation, providing an unprecedented versatility and variety of methodologies for ultrafast spectroscopy and nonlinear optics.

Driven by the primary 3FST sources outlined in Section 3, secondary sources of femtosecond light are likely to outperform their predecessors based on 2FST in several respects. Not only are 3FST-based secondary sources likely to exceed the power of their 2FST-based predecessors by orders of magnitude, but they may also dramatically extend their spectral coverage. As an example, we have scrutinized the capability of multiterawatt, multi-octave light transients to extend the photon energy frontier of attosecond pulses to several kiloelectron volts, to the boundary of the regime of hard x rays. With the preoptimized waveform presented in Fig. 13(d), our numerical simulations of HHG, based on the strong field approximation [205] in helium [see caption of Fig. 13(e) for details] show that synthesized multi-octave transients are superior to few-cycle pulses in pushing the frontiers of HHG into the regime of hard x rays. As a matter of fact, our preoptimized subcycle transients substantially increase the photon energy of the cutoff harmonics as compared to those generated by a 5 fs Gaussian pulse of identical peak power. Our preliminary study indicates that 3FST will be beneficial for extending the frontiers of attosecond science into the x-ray regime.

1FST provided real-time access to a wealth of microscopic phenomena for the first time and created the technological basis for the birth of femtochemistry, allowing direct insight into the making and breaking of chemical bonds. 2FST has also created entirely new research fields and technologies, such as laser-driven accelerators and attosecond science. 3FST holds promise for consequences of comparable impact. One of them may be the recording of movies of any microscopic motion outside the atomic core via attosecond x-ray diffraction.

5. FUNDING INFORMATION

Center for Advanced Laser Applications (CALA); German Federal Ministry of Education and Research (BMBF); Max-Planck-Institute of Quantum Optics (MPQ); Munich Center for Advanced Photonics (MAP); Deutsche Forschungsgemeinschaft (DFG) (EXC-158).

DEDICATION

This paper is dedicated to Gerard Mourou on the occasion of his 70th birthday. His invention, chirped-pulse amplification, laid the groundwork for both second-generation and third-generation femtosecond technology, and thereby for all fields of science relying on intense laser light. Thank you, Gerard!

ACKNOWLEDGMENTS

The authors acknowledge both direct and indirect contributions from a number of colleagues at MPQ and LMU. Most importantly, the pioneering work of Stefan Karsch, László Veisz, and co-workers in the field of high-power OPCPA has led to relevant progress and insight on which the current work draws. We thank Christian Hackenberger for preparing the graphical illustrations for this paper.

See Supplement 1 for supporting content.

REFERENCES AND NOTES

1. E. P. Ippen, C. V. Shank, and A. Dienes, "Passive mode locking of the cw dye laser," Appl. Phys. Lett. **21**, 348–350 (1972).
2. J. P. Letouzey and S. O. Sari, "Continuous pulse train dye laser using an open flowing passive absorber," Appl. Phys. Lett. **23**, 311–313 (1973).
3. C. V. Shank and E. P. Ippen, "Subpicosecond kilowatt pulses from a mode-locked cw dye laser," Appl. Phys. Lett. **24**, 373–375 (1974).
4. R. L. Fork, B. I. Greene, and C. V. Shank, "Generation of optical pulses shorter than 0.1 psec by colliding pulse mode-locking," Appl. Phys. Lett. **38**, 671–672 (1981).
5. W. Dietel, E. Dopel, D. Kuhlke, and B. Wilhelmi, "Pulses in the femtosecond range from a cw dye ring laser in the colliding pulse mode-locking (CPM) regime with down-chirp," Opt. Commun. **43**, 433–436 (1982).
6. W. Dietel, J. J. Fontaine, and J. C. Diels, "Intracavity pulse-compression with glass: a new method of generating pulses shorter than 60 fsec," Opt. Lett. **8**, 4–6 (1983).
7. J. A. Valdmanis, R. L. Fork, and J. P. Gordon, "Generation of optical pulses as short as 27 femtoseconds directly from a laser balancing self-phase modulation, group-velocity dispersion, saturable absorption, and saturable gain," Opt. Lett. **10**, 131–133 (1985).
8. W. H. Knox, M. C. Downer, R. L. Fork, and C. V. Shank, "Amplified femtosecond optical pulses and continuum generation at 5-kHz repetition rate," Opt. Lett. **9**, 552–554 (1984).
9. C. Rolland and P. B. Corkum, "Amplification of 70-fs-pulses in a high repetition rate XeCl pumped dye-laser amplifier," Opt. Commun. **59**, 64–68 (1986).
10. W. Kaiser, D. H. Auston, K. B. Eisenthal, R. M. Hochstrasser, C. K. Johnson, A. Laubereau, D. Linde, A. von der Seilmeier, C. V. Shank, and W. Zinth, *Ultrashort Laser Pulses: Generation and Applications* (Springer, 1993).
11. A. H. Zewail, "Femtochemistry: atomic-scale dynamics of the chemical bond," J. Phys. Chem. A **104**, 5660–5694 (2000).
12. P. F. Moulton, "Spectroscopic and laser characteristics of Ti-Al_2O_3," J. Opt. Soc. Am. B **3**, 125–133 (1986).
13. V. Petričević, S. K. Gayen, R. R. Alfano, K. Yamagishi, H. Anzai, and Y. Yamaguchi, "Laser action in chromium-doped forsterite," Appl. Phys. Lett. **52**, 1040–1042 (1988).
14. E. Sorokin, S. Naumov, and I. T. Sorokina, "Ultrabroadband infrared solid-state lasers," IEEE J. Sel. Top. Quantum Electron. **11**, 690–712 (2005).
15. D. Strickland and G. Mourou, "Compression of amplified chirped optical pulses," Opt. Commun. **56**, 219–221 (1985).
16. D. E. Spence, P. N. Kean, and W. Sibbett, "60-fsec pulse generation from a self-mode-locked Ti:sapphire laser," Opt. Lett. **16**, 42–44 (1991).
17. S. Backus, C. G. Durfee, G. Mourou, H. C. Kapteyn, and M. M. Murnane, "0.2-TW laser system at 1 kHz," Opt. Lett. **22**, 1256–1258 (1997).
18. Y. Nabekawa, Y. Kuramoto, T. Togashi, T. Sekikawa, and S. Watanabe, "Generation of 0.66-TW pulses at 1 kHz by a Ti:sapphire laser," Opt. Lett. **23**, 1384–1386 (1998).
19. R. Szipöcs, K. Ferencz, C. Spielmann, and F. Krausz, "Chirped multilayer coatings for broad-band dispersion control in femtosecond lasers," Opt. Lett. **19**, 201–203 (1994).
20. M. Nisoli, S. DeSilvestri, O. Svelto, R. Szipöcs, K. Ferencz, C. Spielmann, S. Sartania, and F. Krausz, "Compression of high-energy laser pulses below 5 fs," Opt. Lett. **22**, 522–524 (1997).
21. S. Sartania, Z. Cheng, M. Lenzner, G. Tempea, C. Spielmann, F. Krausz, and K. Ferencz, "Generation of O.1-TW 5-fs optical pulses at a 1-kHz repetition rate," Opt. Lett. **22**, 1562–1564 (1997).
22. F. Krausz and M. Ivanov, "Attosecond physics," Rev. Mod. Phys. **81**, 163–234 (2009).
23. G. A. Mourou, T. Tajima, and S. V. Bulanov, "Optics in the relativistic regime," Rev. Mod. Phys. **78**, 309–371 (2006).
24. Y. Chu, X. Liang, L. Yu, Y. Xu, L. Xu, L. Ma, X. Lu, Y. Liu, Y. Leng, R. Li, and Z. Xu, "High-contrast 2.0 petawatt Ti:sapphire laser system," Opt. Express **21**, 29231–29239 (2013).
25. S. Hädrich, A. Klenke, A. Hoffmann, T. Eidam, T. Gottschall, J. Rothhardt, J. Limpert, and A. Tünnermann, "Nonlinear compression to sub-30-fs, 0.5 mJ pulses at 135 W of average power," Opt. Lett. **38**, 3866–3869 (2013).
26. A. Dubietis, G. Jonusauskas, and A. Piskarskas, "Powerful femtosecond pulse generation by chirped and stretched pulse parametric amplification in BBO crystal," Opt. Commun. **88**, 437–440 (1992).
27. D. Du, X. Liu, G. Korn, J. Squier, and G. Mourou, "Laser-induced breakdown by impact ionization in SiO_2 with pulse widths from 7 ns to 150 fs," Appl. Phys. Lett. **64**, 3071–3073 (1994).
28. B. C. Stuart, M. D. Feit, A. M. Rubenchik, B. W. Shore, and M. D. Perry, "Laser-induced damage in dielectrics with nanosecond to subpicosecond pulses," Phys. Rev. Lett. **74**, 2248–2251 (1995).
29. M. Lenzner, J. Krüger, S. Sartania, Z. Cheng, C. Spielmann, G. Mourou, W. Kautek, and F. Krausz, "Femtosecond optical breakdown in dielectrics," Phys. Rev. Lett. **80**, 4076–4079 (1998).
30. C. Radzewicz, Y. B. Band, G. W. Pearson, and J. S. Krasinski, "Short pulse nonlinear frequency conversion without group-velocity-mismatch broadening," Opt. Commun. **117**, 295–302 (1995).
31. S. M. Saltiel, K. Koynov, B. Agate, and W. Sibbett, "Second-harmonic generation with focused beams under conditions of large group-velocity mismatch," J. Opt. Soc. Am. B **21**, 591–598 (2004).
32. C. Y. Chien, G. Korn, J. S. Coe, J. Squier, and G. Mourou, "Highly efficient second-harmonic generation of ultraintense Nd-glass laser pulses," Opt. Lett. **20**, 353–355 (1995).
33. P. Rußbüldt, J. Weitenberg, T. Sartorius, G. Rotarius, H. D. Hoffmann, and R. Poprawe, "Ytterbium Innoslab amplifiers—the high average power approach of ultrafast lasers," AIP Conf. Proc. **1462**, 120–123 (2012).
34. P. Russbueldt, T. Mans, G. Rotarius, J. Weitenberg, H. D. Hoffmann, and R. Poprawe, "400 W Yb:YAG Innoslab fs-amplifier," Opt. Express **17**, 12230–12245 (2009).
35. O. G. Peterson, S. A. Tuccio, and B. B. Snavely, "CW operation of an organic dye solution laser," Appl. Phys. Lett. **17**, 245–247 (1970).
36. M. DiDomenico, "Small-signal analysis of internal (coupling-type) modulation of lasers," J. Appl. Phys. **35**, 2870–2876 (1964).
37. L. E. Hargrove, R. L. Fork, and M. A. Pollack, "Locking of He-Ne laser modes induced by synchronous intracavity modulation," Appl. Phys. Lett. **5**, 4–5 (1964).
38. A. Yariv, "Internal modulation in multimode laser oscillators," J. Appl. Phys. **36**, 388–391 (1965).
39. E. P. Ippen and C. V. Shank, "Dynamic spectroscopy and subpicosecond pulse compression," Appl. Phys. Lett. **27**, 488–490 (1975).
40. J. C. Diels, E. Vanstryland, and G. Benedict, "Generation and measurement of 200 femtosecond optical pulses," Opt. Commun. **25**, 93–96 (1978).
41. E. B. Treacy, "Measurement of picosecond pulse substructure using compression techniques," Appl. Phys. Lett. **14**, 112–114 (1969).
42. R. L. Fork, C. H. B. Cruz, P. C. Becker, and C. V. Shank, "Compression of optical pulses to six femtoseconds by using cubic phase compensation," Opt. Lett. **12**, 483–485 (1987).

43. C. V. Shank, "Generation of ultrashort optical pulses," Top. Appl. Phys. **60**, 5–34 (1988).
44. J. C. Diels, "Femtosecond dye lasers," in *Dye Laser Principles*, F. J. Duarte and L. W. Hillman, eds. (Academic, 1990), Chap. 3, pp. 41–132.
45. P. M. W. French, "The generation of ultrashort laser pulses," Rep. Prog. Phys. **58**, 169–262 (1995).
46. U. Keller, G. W. Thooft, W. H. Knox, and J. E. Cunningham, "Femtosecond pulses from a continuously self-starting passively mode-locked Ti:sapphire laser," Opt. Lett. **16**, 1022–1024 (1991).
47. L. Spinelli, B. Couillaud, N. Goldblatt, and D. K. Negus, "Starting and generation of sub-100 fs pulses in Ti:Al_2O_3 by self-focusing," in *Conference on Lasers and Electro-Optics*, J. Bufton, A. Glass, T. Hsu, and W. Krupke, eds., Vol. **10** of OSA Technical Digest (Optical Society of America, 1991), paper CPD7.
48. M. Piche, "Beam reshaping and self-mode-locking in nonlinear laser resonators," Opt. Commun. **86**, 156–160 (1991).
49. T. Brabec, C. Spielmann, P. F. Curley, and F. Krausz, "Kerr lens mode-locking," Opt. Lett. **17**, 1292–1294 (1992).
50. H. A. Haus, J. G. Fujimoto, and E. P. Ippen, "Analytic theory of additive pulse and Kerr lens mode locking," IEEE J. Quantum Electron. **28**, 2086–2096 (1992).
51. V. P. Kalosha, M. Muller, J. Herrmann, and S. Gatz, "Spatiotemporal model of femtosecond pulse generation in Kerr-lens mode-locked solid-state lasers," J. Opt. Soc. Am. B **15**, 535–550 (1998).
52. R. Szipöcs, A. Stingl, C. Spielmann, and F. Krausz, "Chirped dielectric mirrors for dispersion control in femtosecond laser systems," Proc. SPIE **2377**, 11–22 (1995).
53. A. Stingl, M. Lenzner, C. Spielmann, F. Krausz, and R. Szipöcs, "Sub-10-fs mirror-dispersion-controlled Ti:sapphire laser," Opt. Lett. **20**, 602–604 (1995).
54. A. Kasper and K. J. Witte, "10-fs pulse generation from a unidirectional Kerr-lens mode-locked Ti:sapphire ring laser," Opt. Lett. **21**, 360–362 (1996).
55. T. Brabec and F. Krausz, "Intense few-cycle laser fields: frontiers of nonlinear optics," Rev. Mod. Phys. **72**, 545–591 (2000).
56. P. Maine, D. Strickland, P. Bado, M. Pessot, and G. Mourou, "Generation of ultrahigh peak power pulses by chirped pulse amplification," IEEE J. Quantum Electron. **24**, 398–403 (1988).
57. J. V. Rudd, G. Korn, S. Kane, J. Squier, G. Mourou, and P. Bado, "Chirped-pulse amplification of 55-fs pulses at a 1-kHz repetition rate in a Ti-Al_2O_3 regenerative amplifier," Opt. Lett. **18**, 2044–2046 (1993).
58. O. E. Martinez, "Design of high-power ultrashort pulse amplifiers by expansion and recompression," IEEE J. Quantum Electron. **23**, 1385–1387 (1987).
59. C. P. J. Barty, G. Korn, F. Raksi, A. C. Tien, K. R. Wilson, V. V. Yakovlev, C. Rose-Petruck, J. Squier, and K. Yamakawa, "Regenerative pulse shaping and amplification of ultrabroadband optical pulses," Opt. Lett. **21**, 219–221 (1996).
60. M. Hentschel, Z. Cheng, F. Krausz, and C. Spielmann, "Generation of 0.1-TW optical pulses with a single-stage Ti:sapphire amplifier at a 1-kHz repetition rate," Appl. Phys. B **70**, S161–S164 (2000).
61. J. Z. H. Yang and B. C. Walker, "0.09-terawatt pulses with a 31% efficient, kilohertz repetition-rate Ti:sapphire regenerative amplifier," Opt. Lett. **26**, 453–455 (2001).
62. S. Backus, R. Bartels, S. Thompson, R. Dollinger, M. Murnane, and H. Kapteyn, "High efficiency, single-stage, 7 kHz, high average power ultrafast laser system," in *Conference on Lasers and Electro-Optics*, Baltimore, Maryland, 2001.
63. D. M. Gaudiosi, A. L. Lytle, P. Kohl, M. M. Murnane, H. C. Kapteyn, and S. Backus, "11-W average power Ti:sapphire amplifier system using downchirped pulse amplification," Opt. Lett. **29**, 2665–2667 (2004).
64. J. Huve, T. Haarlammert, T. Steinbruck, J. Kutzner, G. Tsilimis, and H. Zacharias, "High-flux high harmonic soft x-ray generation up to 10 kHz repetition rate," Opt. Commun. **266**, 261–265 (2006).
65. T. Imahoko, N. Inoue, K. Takasago, T. Sumiyoshi, H. Sekita, and M. Obara, "Development of a 50 kHz, 13 W Ti:sapphire femtosecond regenerative amplifier," in *Pacific Rim Conference on Lasers and Electro-Optics* (IEEE, 2007), pp. 774–775.
66. S. Chen, M. Chini, H. Wang, C. Yun, H. Mashiko, Y. Wu, and Z. Chang, "Carrier-envelope phase stabilization and control of 1 kHz, 6 mJ, 30 fs laser pulses from a Ti:sapphire regenerative amplifier," Appl. Opt. **48**, 5692–5695 (2009).
67. I. Matsushima, H. Yashiro, and T. Tomie, "10 kHz 40 W Ti:sapphire regenerative ring amplifier," Opt. Lett. **31**, 2066–2068 (2006).
68. M. Nisoli, S. DeSilvestri, and O. Svelto, "Generation of high energy 10 fs pulses by a new pulse compression technique," Appl. Phys. Lett. **68**, 2793–2795 (1996).
69. E. Goulielmakis, M. Schultze, M. Hofstetter, V. S. Yakovlev, J. Gagnon, M. Uiberacker, A. L. Aquila, E. M. Gullikson, D. T. Attwood, R. Kienberger, F. Krausz, and U. Kleineberg, "Single-cycle nonlinear optics," Science **320**, 1614–1617 (2008).
70. A. L. Cavalieri, E. Goulielmakis, B. Horvath, W. Helml, M. Schultze, M. Fieß, V. Pervak, L. Veisz, V. S. Yakovlev, M. Uiberacker, A. Apolonski, F. Krausz, and R. Kienberger, "Intense 1.5-cycle near infrared laser waveforms and their use for the generation of ultrabroadband soft-x-ray harmonic continua," New J. Phys. **9**, 242 (2007).
71. S. Bohman, A. Suda, T. Kanai, S. Yamaguchi, and K. Midorikawa, "Generation of 5.0 fs, 5.0 mJ pulses at 1 kHz using hollow-fiber pulse compression," Opt. Lett. **35**, 1887–1889 (2010).
72. W. Schweinberger, A. Sommer, E. Bothschafter, J. Li, F. Krausz, R. Kienberger, and M. Schultze, "Waveform-controlled near-single-cycle milli-joule laser pulses generate sub-10 nm extreme ultraviolet continua," Opt. Lett. **37**, 3573–3575 (2012).
73. U. Morgner, F. X. Kartner, S. H. Cho, Y. Chen, H. A. Haus, J. G. Fujimoto, E. P. Ippen, V. Scheuer, G. Angelow, and T. Tschudi, "Sub-two-cycle pulses from a Kerr-lens mode-locked Ti:sapphire laser," Opt. Lett. **24**, 411–413 (1999).
74. C. C. Wang and G. W. Racette, "Measurement of parametric gain accompanying optical difference frequency generation," Appl. Phys. Lett. **6**, 169–171 (1965).
75. S. E. Harris, M. K. Oshman, and R. L. Byer, "Observation of tunable optical parametric fluorescence," Phys. Rev. Lett. **18**, 732–734 (1967).
76. C. Chen, B. Wu, A. Jiang, and G. You, "A new-type ultraviolet SHG crystal: β-BaB_2O_4," Sci. Sin. Ser. B **28**, 235–243 (1985).
77. T. Wilhelm, J. Piel, and E. Riedle, "Sub-20-fs pulses tunable across the visible from a blue-pumped single-pass noncollinear parametric converter," Opt. Lett. **22**, 1494–1496 (1997).
78. E. Riedle, M. Beutter, S. Lochbrunner, J. Piel, S. Schenkl, S. Sporlein, and W. Zinth, "Generation of 10 to 50 fs pulses tunable through all of the visible and the NIR," Appl. Phys. B **71**, 457–465 (2000).
79. R. Butkus, R. Danielius, A. Dubietis, A. Piskarskas, and A. Stabinis, "Progress in chirped pulse optical parametric amplifiers," Appl. Phys. B **79**, 693–700 (2004).
80. A. Dubietis, R. Butkus, and A. P. Piskarskas, "Trends in chirped pulse optical parametric amplification," IEEE J. Sel. Top. Quantum Electron. **12**, 163–172 (2006).
81. S. Witte and K. S. E. Eikema, "Ultrafast optical parametric chirped-pulse amplification," IEEE J. Sel. Top. Quantum Electron. **18**, 296–307 (2012).
82. A. Vaupel, N. Bodnar, B. Webb, L. Shah, and M. Richardson, "Concepts, performance review, and prospects of table-top, few-cycle optical parametric chirped-pulse amplification," Opt. Eng. **53**, 051507 (2014).
83. G. Cerullo and S. De Silvestri, "Ultrafast optical parametric amplifiers," Rev. Sci. Instrum. **74**, 1–18 (2003).
84. A. Baltuska, T. Fuji, and T. Kobayashi, "Visible pulse compression to 4 fs by optical parametric amplification and programmable dispersion control," Opt. Lett. **27**, 306–308 (2002).
85. D. Herrmann, L. Veisz, R. Tautz, F. Tavella, K. Schmid, V. Pervak, and F. Krausz, "Generation of sub-three-cycle, 16 TW light pulses by using noncollinear optical parametric chirped-pulse amplification," Opt. Lett. **34**, 2459–2461 (2009).

86. I. N. Ross, P. Matousek, M. Towrie, A. J. Langley, and J. L. Collier, "The prospects for ultrashort pulse duration and ultrahigh intensity using optical parametric chirped pulse amplifiers," Opt. Commun. **144**, 125–133 (1997).
87. I. N. Ross, P. Matousek, G. H. C. New, and K. Osvay, "Analysis and optimization of optical parametric chirped pulse amplification," J. Opt. Soc. Am. B **19**, 2945–2956 (2002).
88. C. N. Danson, P. A. Brummitt, R. J. Clarke, J. L. Collier, B. Fell, A. J. Frackiewicz, S. Hawkes, C. Hernandez-Gomez, P. Holligan, M. H. R. Hutchinson, A. Kidd, W. J. Lester, I. O. Musgrave, D. Neely, D. R. Neville, P. A. Norreys, D. A. Pepler, C. Reason, W. Shaikh, T. B. Winstone, R. W. W. Wyatt, and B. E. Wyborn, "Vulcan petawatt: design, operation and interactions at 5×10^{20} Wcm^{-2}," Laser Part. Beams **23**, 87–93 (2005).
89. O. V. Chekhlov, J. L. Collier, I. N. Ross, P. K. Bates, M. Notley, C. Hernandez-Gomez, W. Shaikh, C. N. Danson, D. Neely, P. Matousek, S. Hancock, and L. Cardoso, "35 J broadband femtosecond optical parametric chirped pulse amplification system," Opt. Lett. **31**, 3665–3667 (2006).
90. V. V. Lozhkarev, G. I. Freidman, V. N. Ginzburg, E. V. Katin, E. A. Khazanov, A. V. Kirsanov, G. A. Luchinin, A. N. Mal'shakov, M. A. Martyanov, O. V. Palashov, A. K. Poteomkin, A. M. Sergeev, A. A. Shaykin, and I. V. Yakovlev, "Compact 0.56 petawatt laser system based on optical parametric chirped pulse amplification in KD*P crystals," Laser Phys. Lett. **4**, 421–427 (2007).
91. Z. Major, S. Trushin, I. Ahmad, M. Siebold, C. Wandt, S. Klingebiel, T.-J. Wang, J. A. Fülöp, A. Henig, S. Kruber, R. Weingartner, A. Popp, J. Osterhoff, R. Hörlein, J. Hein, V. Pervak, A. Apolonski, F. Krausz, and S. Karsch, "Basic concepts and current status of the petawatt field synthesizer—a new approach to ultrahigh field generation," Rev. Laser Eng. **37**, 431–436 (2009).
92. O. Novak, M. Divoky, H. Turcicova, and P. Straka, "Design of a petawatt optical parametric chirped pulse amplification upgrade of the kilojoule iodine laser PALS," Laser Part. Beams **31**, 211–218 (2013).
93. J. Rothhardt, S. Demmler, S. Hadrich, J. Limpert, and A. Tunnermann, "Octave-spanning OPCPA system delivering CEP-stable few-cycle pulses and 22 W of average power at 1 MHz repetition rate," Opt. Express **20**, 10870–10878 (2012).
94. S. Adachi, N. Ishii, T. Kanai, A. Kosuge, J. Itatani, Y. Kobayashi, D. Yoshitomi, K. Torizuka, and S. Watanabe, "5-fs, multi-mJ, CEP-locked parametric chirped-pulse amplifier pumped by a 450-nm source at 1 kHz," Opt. Express **16**, 14341–14352 (2008).
95. D. J. Bradley and W. Sibbett, "Streak-camera studies of picosecond pulses from a mode-locked Nd: glass laser," Opt. Commun. **9**, 17–20 (1973).
96. T. R. Royt, "Passive mode-locking of the Nd-glass oscillator at high repetition rate with thermally compensated phosphate glasses," Opt. Commun. **35**, 271–276 (1980).
97. L. S. Goldberg, P. E. Schoen, and M. J. Marrone, "Repetitively pulsed mode-locked Nd:phosphate glass laser oscillator-amplifier system," Appl. Opt. **21**, 1474–1477 (1982).
98. S. Tokita, J. Kawanaka, Y. Izawa, M. Fujita, and T. Kawashima, "23.7-W picosecond cryogenic-Yb:YAG multipass amplifier," Opt. Express **15**, 3955–3961 (2007).
99. P. Russbueldt, T. Mans, J. Weitenberg, H. D. Hoffmann, and R. Poprawe, "Compact diode-pumped 1.1 kW Yb:YAG Innoslab femtosecond amplifier," Opt. Lett. **35**, 4169–4171 (2010).
100. T. Eidam, S. Hanf, E. Seise, T. V. Andersen, T. Gabler, C. Wirth, T. Schreiber, J. Limpert, and A. Tünnermann, "Femtosecond fiber CPA system emitting 830 W average output power," Opt. Lett. **35**, 94–96 (2010).
101. K.-H. Hong, J. T. Gopinath, D. Rand, A. M. Siddiqui, S.-W. Huang, E. Li, B. J. Eggleton, J. D. Hybl, T. Y. Fan, and F. X. Kärtner, "High-energy, kHz-repetition-rate, ps cryogenic Yb:YAG chirped-pulse amplifier," Opt. Lett. **35**, 1752–1754 (2010).
102. J. Rothhardt, S. Hädrich, H. Carstens, N. Herrick, S. Demmler, J. Limpert, and A. Tünnermann, "1 MHz repetition rate hollow fiber pulse compression to sub-100-fs duration at 100 W average power," Opt. Lett. **36**, 4605–4607 (2011).
103. D. A. Rand, S. E. J. Shaw, J. R. Ochoa, D. J. Ripin, A. Taylor, T. Y. Fan, H. Martin, S. Hawes, J. Zhang, S. Sarkisyan, E. Wilson, and P. Lundquist, "Picosecond pulses from a cryogenically cooled, composite amplifier using Yb:YAG and Yb:GSAG," Opt. Lett. **36**, 340–342 (2011).
104. K. Kowalewski, J. Zembek, V. Envid, and D. C. Brown, "201 W picosecond green laser using a mode-locked fiber laser driven cryogenic Yb:YAG amplifier system," Opt. Lett. **37**, 4633–4635 (2012).
105. K. F. Wall, D. E. Miller, and T. Y. Fan, "Cryo-Yb:YAG lasers for next-generation photoinjector applications," Proc. SPIE **8235**, 823512 (2012).
106. A. Klenke, S. Breitkopf, M. Kienel, T. Gottschall, T. Eidam, S. Hädrich, J. Rothhardt, J. Limpert, and A. Tünnermann, "530 W, 1.3 mJ, four-channel coherently combined femtosecond fiber chirped-pulse amplification system," Opt. Lett. **38**, 2283–2285 (2013).
107. C. Jauregui, J. Limpert, and A. Tünnermann, "High-power fibre lasers," Nat. Photonics **7**, 861–867 (2013).
108. R. Riedel, A. Stephanides, M. J. Prandolini, B. Gronloh, B. Jungbluth, T. Mans, and F. Tavella, "Power scaling of supercontinuum seeded megahertz-repetition rate optical parametric chirped pulse amplifiers," Opt. Lett. **39**, 1422–1424 (2014).
109. B. A. Reagan, C. Baumgarten, K. Wernsing, H. Bravo, M. Woolston, A. Curtis, F. J. Furch, B. Luther, D. Patel, C. Menoni, and J. J. Rocca, "1 Joule, 100 Hz repetition rate, picosecond CPA laser for driving high average power soft x-ray lasers," in *CLEO*, OSA Technical Digest (online) (Optical Society of America, 2014), paper SM1F.4.
110. M. Schulz, R. Riedel, A. Willner, T. Mans, C. Schnitzler, P. Russbueldt, J. Dolkemeyer, E. Seise, T. Gottschall, S. Hädrich, S. Duesterer, H. Schlarb, J. Feldhaus, J. Limpert, B. Faatz, A. Tünnermann, J. Rossbach, M. Drescher, and F. Tavella, "Yb:YAG Innoslab amplifier: efficient high repetition rate subpicosecond pumping system for optical parametric chirped pulse amplification," Opt. Lett. **36**, 2456–2458 (2011).
111. G. Mourou, B. Brocklesby, T. Tajima, and J. Limpert, "The future is fibre accelerators," Nat. Photonics **7**, 258–261 (2013).
112. S. Breitkopf, "A path to terawatt peak-power fibre laser systems" (submitted).
113. G. Huber, C. Kränkel, and K. Petermann, "Solid-state lasers: status and future," J. Opt. Soc. Am. B **27**, B93–B105 (2010).
114. D. J. Richardson, J. Nilsson, and W. A. Clarkson, "High power fiber lasers: current status and future perspectives," J. Opt. Soc. Am. B **27**, B63–B92 (2010).
115. J. W. Dawson, J. K. Crane, M. J. Messerly, M. A. Prantil, P. H. Pax, A. K. Sridharan, G. S. Allen, D. R. Drachenberg, H. H. Phan, J. E. Heebner, C. A. Ebbers, R. J. Beach, E. P. Hartouni, C. W. Siders, T. M. Spinka, C. P. J. Barty, A. J. Bayramian, L. C. Haefner, F. Albert, W. H. Lowdermilk, A. M. Rubenchik, and R. E. Bonanno, "High average power lasers for future particle accelerators," AIP Conf. Proc. **1507**, 147–153 (2012).
116. M. E. Fermann and I. Hartl, "Ultrafast fibre lasers," Nat. Photonics **7**, 868–874 (2013).
117. A. Giesen, H. Hügel, A. Voss, K. Wittig, U. Brauch, and H. Opower, "Scalable concept for diode-pumped high-power solid-state lasers," Appl. Phys. B **58**, 365–372 (1994).
118. A. Giesen and J. Speiser, "Fifteen years of work on thin-disk lasers: results and scaling laws," IEEE J. Sel. Top. Quantum Electron. **13**, 598–609 (2007).
119. D. Kouznetsov, J.-F. Bisson, and K. Ueda, "Scaling laws of disk lasers," Opt. Mater. **31**, 754–759 (2009).
120. J. Speiser, "Scaling of thin-disk lasers—influence of amplified spontaneous emission," J. Opt. Soc. Am. B **26**, 26–35 (2009).
121. S. V. Marchese, C. R. E. Baer, R. Peters, C. Kränkel, A. G. Engqvist, M. Golling, D. J. H. C. Maas, K. Petermann, T. Südmeyer, G. Huber, and U. Keller, "Efficient femtosecond high power Yb:Lu_2O_3 thin disk laser," Opt. Express **15**, 16966–16971 (2007).

122. C. R. E. Baer, C. Kränkel, C. J. Saraceno, O. H. Heckl, M. Golling, T. Südmeyer, R. Peters, K. Petermann, G. Huber, and U. Keller, "Femtosecond Yb:Lu_2O_3 thin disk laser with 63 W of average power," Opt. Lett. **34**, 2823–2825 (2009).
123. S. Ricaud, A. Jaffres, P. Loiseau, B. Viana, B. Weichelt, M. Abdou-Ahmed, A. Voss, T. Graf, D. Rytz, M. Delaigue, E. Mottay, P. Georges, and F. Druon, "Yb:$CaGdAlO_4$ thin-disk laser," Opt. Lett. **36**, 4134–4136 (2011).
124. W. P. Latham, A. Lobad, T. C. Newell, and D. Stalnaker, "6.5 kW, Yb:YAG ceramic thin disk laser," AIP Conf. Proc. **1278**, 758–764 (2010).
125. M. Suzuki, H. Kiriyama, I. Daito, Y. Ochi, H. Okada, M. Sato, Y. Tamaoki, T. Yoshii, J. Maeda, S. Matsuoka, H. Kan, P. R. Bolton, A. Sugiyama, K. Kondo, and S. Kawanishi, "Hundred mJ, sub-picoseconds, high temporal contrast OPCPA/Yb:YAG ceramic thin disk hybrid laser system," Appl. Phys. B **105**, 181–184 (2011).
126. J. Mende, G. Spindler, J. Speiser, W. L. Bohn, and A. Giesen, "Mode dynamics and thermal lens effects of thin-disk lasers," Proc. SPIE **6871**, 68710M (2008).
127. A. Killi, C. Stolzenburg, I. Zawischa, D. Sutter, J. Kleinbauer, S. Schad, R. Brockmann, S. Weiler, J. Neuhaus, S. Kalfhues, E. Mehner, D. Bauer, H. Schlueter, and C. Schmitz, "The broad applicability of the disk laser principle: from CW to ps," Proc. SPIE **7193**, 71931T (2009).
128. A. Antognini, K. Schuhmann, F. D. Amaro, F. Biraben, A. Dax, A. Giesen, T. Graf, T. W. Hansch, P. Indelicato, L. Julien, C.-Y. Kao, P. E. Knowles, F. Kottmann, E. Le Bigot, Y.-W. Liu, L. Ludhova, N. Moschuring, F. Mulhauser, T. Nebel, F. Nez, P. Rabinowitz, C. Schwob, D. Taqqu, and R. Pohl, "Thin-disk Yb:YAG oscillator-amplifier laser, ASE, and effective Yb:YAG lifetime," IEEE J. Quantum Electron. **45**, 993–1005 (2009).
129. H. Furuse, H. Chosrowjan, J. Kawanaka, N. Miyanaga, M. Fujita, and Y. Izawa, "ASE and parasitic lasing in thin disk laser with anti-ASE cap," Opt. Express **21**, 13118–13124 (2013).
130. D. Bauer, I. Zawischa, D. H. Sutter, A. Killi, and T. Dekorsy, "Mode-locked Yb:YAG thin-disk oscillator with 41 μJ pulse energy at 145 W average infrared power and high power frequency conversion," Opt Express **20**, 9698–9704 (2012).
131. S. Ricaud, A. Jaffres, K. Wentsch, A. Suganuma, B. Viana, P. Loiseau, B. Weichelt, M. Abdou-Ahmed, A. Voss, T. Graf, D. Rytz, C. Hönninger, E. Mottay, P. Georges, and F. Druon, "Femtosecond Yb:$CaGdAlO_4$ thin-disk oscillator," Opt. Lett. **37**, 3984–3986 (2012).
132. O. Pronin, J. Brons, C. Grasse, V. Pervak, G. Boehm, M. C. Amann, A. Apolonski, V. L. Kalashnikov, and F. Krausz, "High-power Kerr-lens mode-locked Yb:YAG thin-disk oscillator in the positive dispersion regime," Opt. Lett. **37**, 3543–3545 (2012).
133. C. J. Saraceno, F. Emaury, C. Schriber, M. Hoffmann, M. Golling, T. Südmeyer, and U. Keller, "Ultrafast thin-disk laser with 80 μJ pulse energy and 242 W of average power," Opt. Lett. **39**, 9–12 (2014).
134. C. Teisset, M. Schultze, R. Bessing, M. Häfner, J. Rauschenberger, D. Sutter, and T. Metzger, "Picosecond thin-disk regenerative amplifier with high average power for pumping optical parametric amplifiers," in *CLEO*, OSA Postdeadline Paper Digest (online) (Optical Society of America, 2013), paper CTh5C.6.
135. J.-P. Negel, A. Voss, M. A. Ahmed, D. Bauer, D. Sutter, A. Killi, and T. Graf, "1.1 kW average output power from a thin-disk multipass amplifier for ultrashort laser pulses," Opt. Lett. **38**, 5442–5445 (2013).
136. H. Fattahi, C. Skrobol, M. Ueffing, Y. Deng, A. Schwarz, Y. Kida, V. Pervak, T. Metzger, Z. Major, and F. Krausz, "High efficiency, multi-mJ, sub 10 fs, optical parametric amplifier at 3 kHz," in *Conference on Lasers and Electro-Optics*, OSA Technical Digest (online) (Optical Society of America, 2012), paper CTh1N.6.
137. J. Aus der Au, G. J. Spuhler, T. Südmeyer, R. Paschotta, R. Hovel, M. Moser, S. Erhard, M. Karszewski, A. Giesen, and U. Keller, "16.2-W average power from a diode-pumped femtosecond Yb: YAG thin disk laser," Opt. Lett. **25**, 859–861 (2000).
138. C. J. Saraceno, F. Emaury, O. H. Heckl, C. R. E. Baer, M. Hoffmann, C. Schriber, M. Golling, T. Südmeyer, and U. Keller, "275 W average output power from a femtosecond thin disk oscillator operated in a vacuum environment," Opt. Express **20**, 23535–23541 (2012).
139. S. V. Marchese, C. R. Baer, A. G. Engqvist, S. Hashimoto, D. J. Maas, M. Golling, T. Sudmeyer, and U. Keller, "Femtosecond thin disk laser oscillator with pulse energy beyond the 10-microjoule level," Opt Express **16**, 6397–6407 (2008).
140. J. Brons, V. Pervak, E. Fedulova, M. Seidel, D. Bauer, D. Sutter, V. L. Kalashnikov, A. Apolonski, O. Pronin, and F. Krausz, "Power-scaling of Kerr-lens mode-locked Yb:YAG thin-disk oscillators," in *CLEO*, OSA Technical Digest (online) (Optical Society of America, 2014), paper SM4F.7.
141. A. Diebold, F. Emaury, C. Schriber, M. Golling, C. J. Saraceno, T. Südmeyer, and U. Keller, "SESAM mode-locked Yb:$CaGdAlO_4$ thin disk laser with 62 fs pulse generation," Opt. Lett. **38**, 3842–3845 (2013).
142. C. J. Saraceno, C. Schriber, M. Mangold, M. Hoffmann, O. H. Heckl, C. R. Baer, M. Golling, T. Südmeyer, and U. Keller, "SESAMs for high-power oscillators: design guidelines and damage thresholds," IEEE J. Sel. Top. Quantum Electron. **18**, 29–41 (2012).
143. O. Pronin, J. Brons, C. Grasse, V. Pervak, G. Boehm, M. C. Amann, V. L. Kalashnikov, A. Apolonski, and F. Krausz, "High-power 200 fs Kerr-lens mode-locked Yb:YAG thin-disk oscillator," Opt. Lett. **36**, 4746–4748 (2011).
144. O. Pronin, M. Seidel, F. Lücking, J. Brons, V. Pervak, A. Apolonski, T. Udem, and F. Krausz, "Next-generation source of waveform-controlled light" (submitted).
145. C. Hönninger, I. Johannsen, M. Moser, G. Zhang, A. Giesen, and U. Keller, "Diode-pumped thin-disk Yb:YAG regenerative amplifier," Appl. Phys. B **65**, 423–426 (1997).
146. T. Metzger, C. Y. Teisset, and F. Krausz, "High-repetition-rate picosecond pump laser based on a Yb:YAG disk amplifier for optical parametric amplification," in *Advanced Solid-State Photonics*, OSA Technical Digest Series (CD) (Optical Society of America, 2008), paper TuA2.
147. C. Teisset, M. Schultze, R. Bessing, M. Haefner, S. Prinz, D. Sutter, and T. Metzger, "300 W picosecond thin-disk regenerative amplifier at 10 kHz repetition rate," in *Advanced Solid-State Lasers Congress Postdeadline*, OSA Postdeadline Paper Digest (online) (Optical Society of America, 2013), paper JTh5A.1.
148. J. Tuemmler, R. Jung, T. Nubbemeyer, I. Will, and W. Sandner, "Providing thin-disk technology for high laser pulse energy at high average power," in *Frontiers in Optics 2011/Laser Science XXVII*, OSA Technical Digest (Optical Society of America, 2011), paper FThB3.
149. M. Schulz, H. Hoeppner, M. Temme, R. Riedel, B. Faatz, M. J. Prandolini, M. Drescher, and F. Tavella, "14 kilowatt burst average power from 2-stage cascaded Yb:YAG thin-disk multipass amplifier," in *Frontiers in Optics*, OSA Technical Digest (online) (Optical Society of America, 2013), paper FTu4A.2.
150. C. Skrobol, I. Ahmad, S. Klingebiel, C. Wandt, S. A. Trushin, Z. Major, F. Krausz, and S. Karsch, "Broadband amplification by picosecond OPCPA in DKDP pumped at 515 nm," Opt. Express **20**, 4619–4629 (2012).
151. S. Klingebiel, I. Ahmad, C. Wandt, C. Skrobol, S. A. Trushin, Z. Major, F. Krausz, and S. Karsch, "Experimental and theoretical investigation of timing jitter inside a stretcher-compressor setup," Opt. Express **20**, 3443–3455 (2012).
152. T. Miura, K. Takasago, A. Endo, K. Torizuka, and F. Kannari, "Timing stabilization of the 1-kHz femtosecond pulses with active control by means of the spectral-resolved upconversion," in *The 4th Pacific Rim Conference on Lasers and Electro-Optics* (IEEE, 2001), Vol. **2**, pp. 520–521.
153. A. Schwarz, M. Ueffing, Y. Deng, X. Gu, H. Fattahi, T. Metzger, M. Ossiander, F. Krausz, and R. Kienberger, "Active stabilization for optically synchronized optical parametric chirped pulse amplification," Opt. Express **20**, 5557–5565 (2012).

154. S. Prinz, "Sub-2-fs active pump-seed synchronization for OPCPA" (submitted).
155. J. Tümmler, R. Jung, H. Stiel, P. V. Nickles, and W. Sandner, "High-repetition-rate chirped-pulse-amplification thin-disk laser system with joule-level pulse energy," Opt. Lett. **34**, 1378–1380 (2009).
156. J. Tümmler, R. Jung, H. Stiel, P. V. Nickles, and W. Sandner, "High repetition rate diode pumped CPA thin disk laser of the joule class," in *Conference on Lasers and Electro-Optics/International Quantum Electronics Conference*, OSA Technical Digest (CD) (Optical Society of America, 2009), paper CFD4.
157. http://www.mb-berlin.de/de/research/projects/1.2/topics/1_power_disk_laser/.
158. M. Gorjan and T. Metzger, (unpublished).
159. J. Speiser, "Thin disk laser—energy scaling," Laser Phys. **19**, 274–280 (2009).
160. T. Gottwald, C. Stolzenburg, D. Bauer, J. Kleinbauer, V. Kuhn, T. Metzger, S. Schad, D. Sutter, and A. Killi, "Recent disk laser development at Trumpf," Proc. SPIE **8547**, 85470C (2012).
161. M. Kienel, M. Müller, S. Demmler, J. Rothhardt, A. Klenke, T. Eidam, J. Limpert, and A. Tünnermann, "Coherent beam combination of Yb:YAG single-crystal rod amplifiers," Opt. Lett. **39**, 3278–3281 (2014).
162. J. Limpert, "Performance scaling of ultrafast laser systems by coherent addition of femtosecond pulses," in *CLEO*, OSA Technical Digest (online) (Optical Society of America, 2014), paper SW3E.3.
163. M. Kienel, A. Klenke, T. Eidam, S. Hädrich, J. Limpert, and A. Tünnermann, "Energy scaling of femtosecond amplifiers using actively controlled divided-pulse amplification," Opt. Lett. **39**, 1049–1052 (2014).
164. D. Herrmann, C. Homann, R. Tautz, M. Scharrer, P. S. J. Russell, F. Krausz, L. Veisz, and E. Riedle, "Approaching the full octave: noncollinear optical parametric chirped pulse amplification with two-color pumping," Opt. Express **18**, 18752–18762 (2010).
165. Alternatively, momentum conservation can also be fulfilled by periodic modulation of some optical property of the nonlinear crystal (quasi-phase matching) instead of exploiting birefringence. Periodically poled crystals are being widely used for this purpose.
166. D. Brida, C. Manzoni, G. Cirmi, M. Marangoni, S. Bonora, P. Villoresi, S. D. Silvestri, and G. Cerullo, "Few-optical-cycle pulses tunable from the visible to the mid-infrared by optical parametric amplifiers," J. Opt. **12**, 013001 (2010).
167. R. Danielius, A. Piskarskas, A. Stabinis, G. P. Banfi, P. Di Trapani, and R. Righini, "Traveling-wave parametric generation of widely tunable, highly coherent femtosecond light pulses," J. Opt. Soc. Am. B **10**, 2222–2232 (1993).
168. T. J. Driscoll, G. M. Gale, and F. Hache, "Ti:sapphire second-harmonic-pumped visible range femtosecond optical parametric oscillator," Opt. Commun. **110**, 638–644 (1994).
169. G. M. Gale, M. Cavallari, T. J. Driscoll, and F. Hache, "Sub-20-fs tunable pulses in the visible from an 82-MHz optical parametric oscillator," Opt. Lett. **20**, 1562–1564 (1995).
170. G. M. Gale, M. Cavallari, and F. Hache, "Femtosecond visible optical parametric oscillator," J. Opt. Soc. Am. B **15**, 702–714 (1998).
171. Optical parametric amplification done in the frequency domain holds promise for relaxing restrictions arising from phase mismatch in OPA.
172. B. E. Schmidt, N. Thiré, M. Boivin, A. Laramée, F. Poitras, G. Lebrun, T. Ozaki, H. Ibrahim, and F. Légaré, "Frequency domain optical parametric amplification," Nat. Commun. **5**, 3643 (2014).
173. M. T. Hassan, A. Wirth, I. Grguraš, A. Moulet, T. T. Luu, J. Gagnon, V. Pervak, and E. Goulielmakis, "Invited Article: Attosecond photonics: synthesis and control of light transients," Rev. Sci. Instrum. **83**, 111301 (2012).
174. S.-W. Huang, G. Cirmi, J. Moses, K.-H. Hong, S. Bhardwaj, J. R. Birge, L.-J. Chen, E. Li, B. J. Eggleton, G. Cerullo, and F. X. Kartner, "High-energy pulse synthesis with sub-cycle waveform control for strong-field physics," Nat. Photonics **5**, 475–479 (2011).
175. S.-W. Huang, G. Cirmi, J. Moses, K.-H. Hong, S. Bhardwaj, J. R. Birge, L.-J. Chen, I. V. Kabakova, E. Li, B. J. Eggleton, G. Cerullo, and F. X. Kärtner, "Optical waveform synthesizer and its application to high-harmonic generation," J. Phys. B **45**, 074009 (2012).
176. C. Manzoni, G. Cerullo, and S. De Silvestri, "Ultrabroadband self-phase-stabilized pulses by difference-frequency generation," Opt. Lett. **29**, 2668–2670 (2004).
177. G. Cerullo, A. Baltuška, O. D. Mücke, and C. Vozzi, "Few-optical-cycle light pulses with passive carrier-envelope phase stabilization," Laser Photon. Rev. **5**, 323–351 (2011).
178. K.-H. Hong, S.-W. Huang, J. Moses, X. Fu, C.-J. Lai, G. Cirmi, A. Sell, E. Granados, P. Keathley, and F. X. Kärtner, "High-energy, phase-stable, ultrabroadband kHz OPCPA at 2.1 μm pumped by a picosecond cryogenic Yb:YAG laser," Opt. Express **19**, 15538–15548 (2011).
179. Y. Deng, A. Schwarz, H. Fattahi, M. Ueffing, X. Gu, M. Ossiander, T. Metzger, V. Pervak, H. Ishizuki, T. Taira, T. Kobayashi, G. Marcus, F. Krausz, R. Kienberger, and N. Karpowicz, "Carrier-envelope-phase-stable, 1.2 mJ, 1.5 cycle laser pulses at 2.1 μm," Opt. Lett. **37**, 4973–4975 (2012).
180. H. Fattahi, A. Schwarz, S. Keiber, and N. Karpowicz, "Efficient, octave-spanning difference-frequency generation using few-cycle pulses in simple collinear geometry," Opt. Lett. **38**, 4216–4219 (2013).
181. D. Kartashov, S. Ališauskas, A. Pugžlys, A. Voronin, A. Zheltikov, M. Petrarca, P. Béjot, J. Kasparian, J.-P. Wolf, and A. Baltuška, "White light generation over three octaves by femtosecond filament at 3.9 μm in argon," Opt. Lett. **37**, 3456–3458 (2012).
182. A. A. Voronin, J. M. Mikhailova, M. Gorjan, Z. Major, and A. M. Zheltikov, "Pulse compression to subcycle field waveforms with split-dispersion cascaded hollow fibers," Opt. Lett. **38**, 4354–4357 (2013).
183. A. Schwarz, "Few-cycle, phase-stable infrared OPCPA," Ph.D. dissertation (LMU, 2014).
184. A. Wirth, M. T. Hassan, I. Grguraš, J. Gagnon, A. Moulet, T. T. Luu, S. Pabst, R. Santra, Z. A. Alahmed, A. M. Azzeer, V. S. Yakovlev, V. Pervak, F. Krausz, and E. Goulielmakis, "Synthesized light transients," Science **334**, 195–200 (2011).
185. O. Razskazovskaya, et al., is preparing an article.
186. S. V. Bulanov, N. M. Naumova, and F. Pegoraro, "Interaction of an ultrashort, relativistically strong laser pulse with an overdense plasma," Phys. Plasmas **1**, 745–757 (1994).
187. R. Lichters, J. Meyer-ter-Vehn, and A. Pukhov, "Short-pulse laser harmonics from oscillating plasma surfaces driven at relativistic intensity," Phys. Plasmas **3**, 3425–3437 (1996).
188. T. Baeva, S. Gordienko, and A. Pukhov, "Theory of high-order harmonic generation in relativistic laser interaction with overdense plasma," Phys. Rev. E **74**, 046404 (2006).
189. G. D. Tsakiris, K. Eidmann, J. Meyer-ter-Vehn, and F. Krausz, "Route to intense single attosecond pulses," New J. Phys. **8**, 19 (2006).
190. P. Heissler, R. Hörlein, J. M. Mikhailova, L. Waldecker, P. Tzallas, A. Buck, K. Schmid, C. M. S. Sears, F. Krausz, L. Veisz, M. Zepf, and G. D. Tsakiris, "Few-cycle driven relativistically oscillating plasma mirrors: a source of intense isolated attosecond pulses," Phys. Rev. Lett. **108**, 235003 (2012).
191. J. M. Mikhailova, M. V. Fedorov, N. Karpowicz, P. Gibbon, V. T. Platonenko, A. M. Zheltikov, and F. Krausz, "Isolated attosecond pulses from laser-driven synchrotron radiation," Phys. Rev. Lett. **109**, 245005 (2012).
192. J. Tate, T. Auguste, H. G. Muller, P. Salières, P. Agostini, and L. F. DiMauro, "Scaling of wave-packet dynamics in an intense midinfrared field," Phys. Rev. Lett. **98**, 013901 (2007).
193. A. D. Shiner, C. Trallero-Herrero, N. Kajumba, H. C. Bandulet, D. Comtois, F. Légaré, M. Giguère, J. C. Kieffer, P. B. Corkum, and D. M. Villeneuve, "Wavelength scaling of high harmonic generation efficiency," Phys. Rev. Lett. **103**, 073902 (2009).

194. F. Krausz and M. I. Stockman, "Attosecond metrology: from electron capture to future signal processing," Nat. Photonics **8**, 205–213 (2014).
195. A. Harth, M. Schultze, T. Lang, T. Binhammer, S. Rausch, and U. Morgner, "Two-color pumped OPCPA system emitting spectra spanning 1.5 octaves from VIS to NIR," Opt. Express **20**, 3076–3081 (2012).
196. C. Manzoni, S. W. Huang, G. Cirmi, P. Farinello, J. Moses, F. X. Kärtner, and G. Cerullo, "Coherent synthesis of ultra-broadband optical parametric amplifiers," Opt. Lett. **37**, 1880–1882 (2012).
197. T. T. Luu, M. T. Hassan, A. Moulet, O. Razskazovskaya, N. Kaprowicz, V. Pervak, F. Krausz, and E. Goulielmakis, "Isolated optical attosecond pulses," in *CLEO*, OSA Technical Digest (online) (Optical Society of America, 2013), paper QF1C.6.
198. M. T. Hassan, "Attosecond control of bound electrons" (submitted).
199. F. X. Kärtner, O. Mücke, G. Cirmi, S. Fang, S.-H. Chia, C. Manzoni, P. Farinello, and G. Cerullo, "High energy sub-cycle optical waveform synthesizer," in *Advanced Solid-State Lasers Congress*, OSA Technical Digest (online) (Optical Society of America, 2013), paper AW2A.1.
200. S. N. Bagayev, V. I. Trunov, E. V. Pestryakov, V. E. Leschenko, S. A. Frolov, and V. A. Vasiliev, "High-intensity femtosecond laser systems based on coherent combining of optical fields," Opt. Spectrosc. **115**, 311–319 (2013).
201. G. M. Rossi, G. Cirmi, S. Fang, S.-H. Chia, O. D. Muecke, F. Kärtner, C. Manzoni, P. Farinello, and G. Cerullo, "Spectro-temporal characterization of all channels in a sub-optical-cycle parametric waveform synthesizer," in *CLEO*, OSA Technical Digest (online) (Optical Society of America, 2014), paper SF1E.3.
202. S. Fang, G. Cirmi, S. H. Chia, O. D. Mucke, F. X. Kartner, C. Manzoni, P. Farinello, and G. Cerullo, "Multi-mJ parametric synthesizer generating two-octave-wide optical waveforms," in *Conference on Lasers and Electro-Optics Pacific Rim* (Optical Society of America, 2013), paper WB3_1.
203. F. Verluise, V. Laude, Z. Cheng, C. Spielmann, and P. Tournois, "Amplitude and phase control of ultrashort pulses by use of an acousto-optic programmable dispersive filter: pulse compression and shaping," Opt. Lett. **25**, 575–577 (2000).
204. T. Binhammer, E. Rittweger, R. Ell, F. X. Kärtner, and U. Morgner, "Prism-based pulse shaper for octave spanning spectra," IEEE J. Quantum Electron. **41**, 1552–1557 (2005).
205. M. Lewenstein, P. Balcou, M. Y. Ivanov, A. L'Huillier, and P. B. Corkum, "Theory of high-harmonic generation by low-frequency laser fields," Phys. Rev. A **49**, 2117–2132 (1994).
206. M. Schultze, C. Y. Teisset, S. Prinz, D. H. Sutter, K. Michel, and T. Metzger, "Highly-efficient, optically synchronized thin disk amplifier for pumping OPCPA at high repetition rates between 100–300 kHz," Solid State Lasers XXIII: Technology and Devices, 2014, to be published.